

POLITECNICO DI TORINO

Master's Degree in
Environmental and Land Engineering



Master's Degree Thesis

**NET CARBON EFFECT OF LAND
USE TRANSFORMATIONS IN
ATLANTIC FOREST BIOME,
EMBRAPA PROTOCOL**

Supervisors

Prof. ELENA COMINO

Dra. JOSILÉIA A. ZANATTA

Author

CLAUDIA USUELLI

March 2023

Summary

Introduction

According to the scientific community, global greenhouse gases emissions can be reduced by forests. Despite the awareness of the important role of these ecosystems, recognition of the ability to mitigate climate change is still poorly measured.

The goal of this study is to present, for the Atlantic forest biome, operational procedures, results and comparison of the carbon sequestration capacity with respect to land use transformations. **The hypothesis** is that different land-use stands will give decreasing carbon capture values in relation to greater anthropization.

Different stands are thus considered, one still covered by the native forest (NAT), one under natural regeneration (REG) and the last devoted to cultivation of Pupunha (PUP).

The Net emissions of the regenerating forest and of the agricultural field are evaluated in relation to the unaltered forest, and computed based on the contributions of: greenhouse gases emitted by soil, soil carbon and carbon stored in vegetation.

The present study is carried out under the auspices of the Brazilian Agricultural Research Corporation, a state-owned research corporation affiliated with the Brazilian Ministry of Agriculture.

The study area is part of the alluvial Atlantic rain forest, in the special usage zone of the Salto Morato Natural Reserve in Guaraqueçaba, Southern Region of Brazil.

Methods

Greenhouse gases emissions

In order to measure gases, static chambers are exploited (figure 1). The experimental design includes three parcels of four chambers each for each forest configuration (NAT/REG/PUP), with four collections taken during the incubation time. 14 field campaigns (from June 2021 to May 2022) are conducted.



Figure 1: Chamber toolkit

The concentrations of CH_4 and N_2O are determined by chromatography. Fluxes are computed as:

$$\text{flow} = \frac{\frac{dC}{dt} \cdot V}{R \cdot T} \cdot P_{atm} \cdot M \quad (1)$$

where: dC = gas concentration in the chamber, V = chamber volume, A = chamber area, T = average temperature inside the chamber, M = gas molar mass. Cumulative emissions are determined to fill temporal gaps between measurements, also accounting for spatial variability.

Soil organic carbon

In order to estimate the SOC, soil density is measured through the 'Kopecky tool' (figure 2), being the dry mass of a sample of known volume.



Figure 2: Kopecky tool

The carbon content measurement makes use of the 'Dutch auger tool' (figure 3).



Figure 3: Dutch auger tool

The experimental design includes 3 parcels for each forest stand, 10 and 8 layers investigated respectively for density and carbon content, until 1 m depth, and 2 rings per layer.

The carbon content is determined in the laboratory by Elementar ®Vario MACRO Cube analyzer. The accumulated carbon is calculated by the equivalent soil mass method.

Forest carbon inventory

The experimental design includes 7 parcels for NAT, 6 for REG and 1 for PUP. Four compartments are investigated: above ground, root, litter, and necromass.

Aboveground compartment. The circumference at breast height, the plant's height, and the species' name are recorded. The biomass is estimated by allometric equations, NAT and REG (Tiepolo et al. 2002), PUP (Ramos et al. 2008). The biomass is converted to carbon assuming 0.47 as mass carbon fraction in biomass (Eggleston 2006).

Root compartment. Existing aerial-root equations are employed, NAT and REG (0.237 root mass/plants mass), PUP (0.29 root mass/plants mass). Biomass carbon fraction is assumed to be 0.47 (Eggleston 2006).

Litter compartment. A 0.35x0.35 m frame is used, randomly dropped six times/parcel; the material remaining inside is collected. The carbon quantification, as for soil, is done by laboratory elements analyzer and computed as:

$$C \text{ (Kg/m}^2\text{)} = \frac{\text{dry weight}}{\text{frame area}} \cdot \%C \quad (2)$$

Necromass compartment. The intercept line method is adopted; for each fragment crossed by the inventory line ($L=25\text{m}$), the diameter at the intersection d and decomposition class are recorded. The total volume (Wagner 1982) is estimated as:

$$V = \left(\frac{1,234}{L}\right) \cdot \sum_{i=1}^i d^2 \quad (3)$$

The weight is the product of V and the density provided by Keller et al. 2004. The carbon content rate assumed is 0.43 KgC/Kg_{DM} (Oliveira Santos 2020).

Total biomass carbon It's the sum of the four compartments depicted above.

Net carbon emission

It's computed as:

$$N_2O + CH_4 - \Delta SOC - \Delta TB \quad (4)$$

where the inputs/outputs are:

- CO_2eq soil-emitted GHGs, represented by N_2O & CH_4 fluxes;
- CO_2eq stored in soil, represented by ΔSOC ;
- CO_2eq sequestered by vegetation, represented by ΔTB .

Results

The mitigation potential is assessed by the global warming potential GWP, CO_2eq of 28 and 265 times for CH_4 and N_2O respectively (Hiraishi et al. 2014).

Greenhouse gases emissions

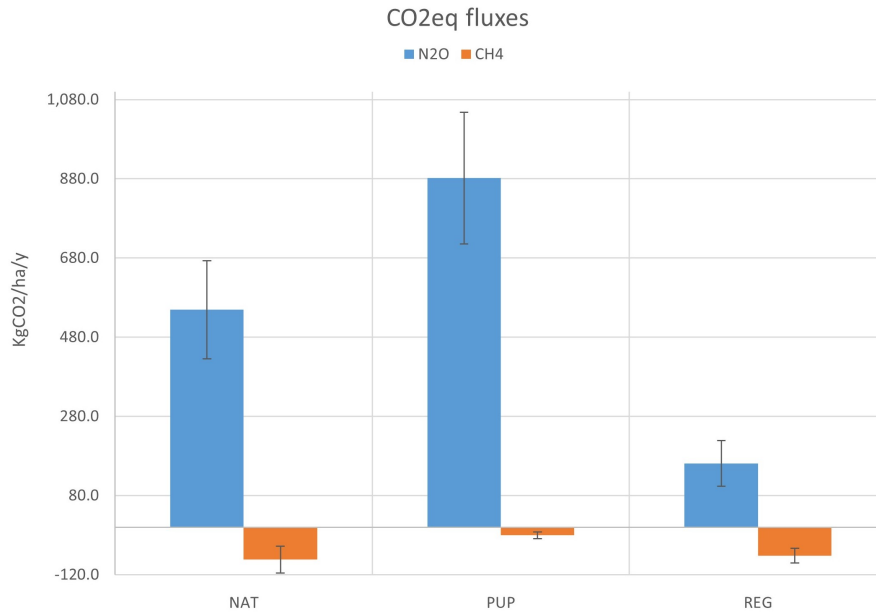


Figure 4: GHGs fluxes in CO_2eq

NAT	N_2O ($KgCO_2/ha/y$)	CH_4 ($KgCO_2/ha/y$)
	549±248	-82±67
PUP	N_2O ($KgCO_2/ha/y$)	CH_4 ($KgCO_2/ha/y$)
	881±332	-20±16
	161±116	-72±37

Table 1: GHGs fluxes in CO_2eq

Comments. • N_2O flux constitutes an emission, CH_4 an influx. • The methane stored in regenerated forest is almost replenished compared to unaltered forest, the same cannot be said for the cultivation.

Soil organic carbon

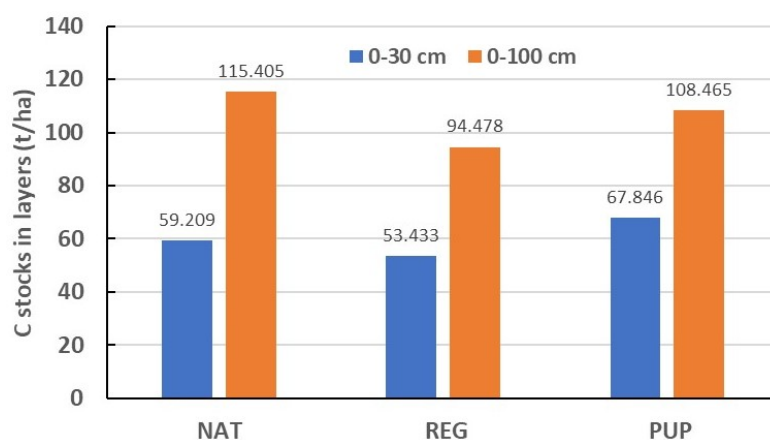


Figure 5: Carbon stock

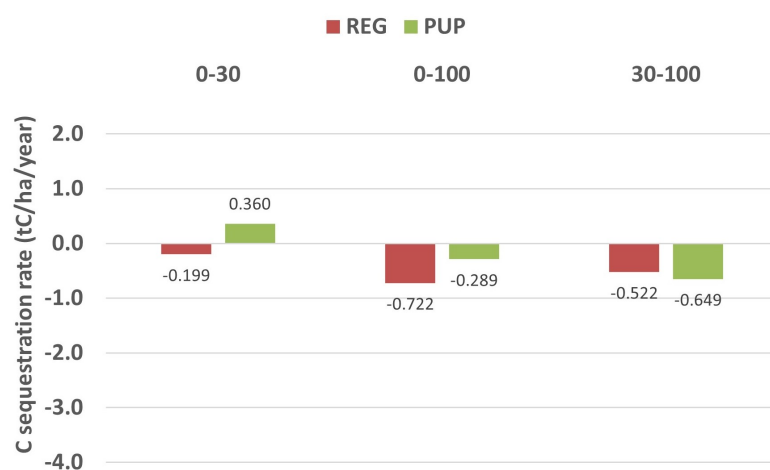


Figure 6: NAT-relative carbon sequestration rate

Land-use	ΔSOC ($KgCO_2/ha/year$)
Regenerated forest	-730
Pupunha culture	1320

Table 2: NAT-relative SOC in CO_2eq

Comments. The hypothesis is only partially confirmed; in 0-100 cm, NAT stores the largest stock of carbon, surprisingly followed by PUP and only after by REG.

Forest carbon inventory

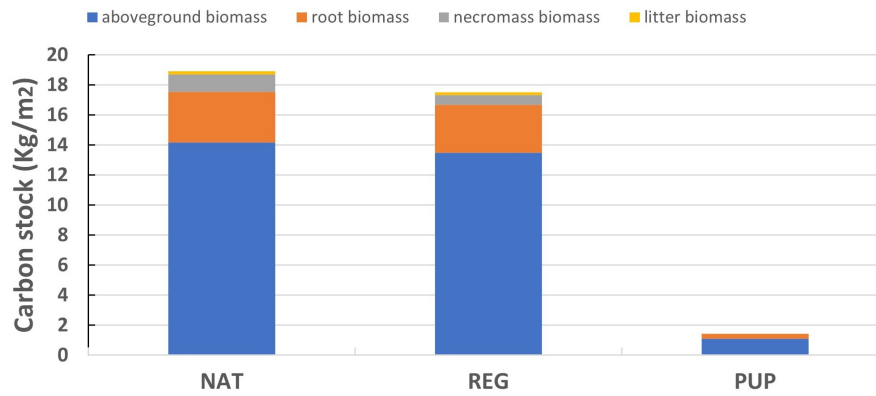


Figure 7: Compartments carbon stock share

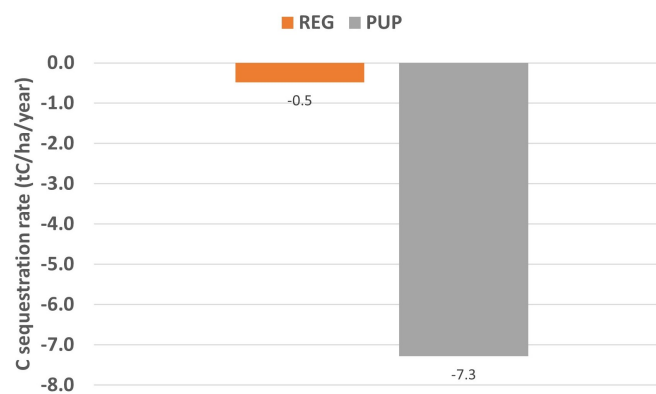


Figure 8: NAT-relative carbon sequestration rate

Land-use	ΔTB ($KgCO_2/ha/year$)
Regenerated forest	-1755
Pupunha culture	-26707

Table 3: NAT-relative TB in CO_2eq

Comments. The hypothesis is confirmed. • REG carbon stock it's almost completely recovered compared to NAT. • PUP carbon stock is very low.

Net carbon emission



Figure 9: NAT-relative carbon sequestration rate

Land-use	Net emission ($KgCO_2/ha/year$)
Native forest	-
Regenerated forest	2575
Pupunha culture	26250

Table 4: Carbon net emissions of natural regenerating forests and palm cultivations, in relation to native forests, in Atlantic forest biome.

Comments. The hypothesis is confirmed. • REG and PUP emit much more in relation to NAT, in particular PUP. • The major contribution comes from the accumulation in Total biomass, the second largest from soil carbon.

Conclusions

Net carbon emissions related to land use transformations are provided (table 4). The interpretation of the outcomes officially confirms the hypothesis of decreasing carbon capture values in relation to greater anthropization. Regenerating forests and palm cultivations turn out to emit much more carbon to the atmosphere in relation to unaltered forests, emphasizing the importance of environmental protection. Additionally, the release from regenerated forests is significantly lower than from cultivated fields, proving the positive impact of natural regeneration. The methodology adopted falls within the Protocol endorsed by Embrapa, offering a comprehensive review, along with some improvements. Future development could be the insertion of these results into the Carbon market system. The significant difference encountered between regenerated forests and cultivated areas could be the driving force of restoration programs; furthermore, it's demonstrated the effectiveness of natural regeneration, whose outcomes are close to those of unaltered forests.

Acknowledgements

To Josileia, my Embrapa supervisor,
for giving enormous trust in my work, for the competencies imparted,
and for the kind availability.

To my University supervisor,
for the invaluable advice and support.

To my family and friends,
for supporting me every step of the way.

Table of Contents

Introduction	1
Methods	2
Greenhouse gases emissions	2
Soil organic carbon	3
Forest carbon inventory	4
Net carbon emission	5
Results	6
Greenhouse gases emissions	6
Soil organic carbon	7
Forest carbon inventory	8
Net carbon emission	9
Conclusions	10
1 Context	15
1.1 Introduction	15
1.2 Research site	18
1.3 Land use history	24
1.4 Parcels configuration	28
1.5 Definitions	29
1.6 Carbon balance	31
2 Greenhouse gases emissions	32
2.1 Introduction	32
2.2 Sampling	32
2.3 Laboratory analysis	41
2.4 Calculus	48
2.5 Results	55
2.6 Result discussion	57
3 Soil organic carbon	58
3.1 Introduction	58
3.2 Sampling	59

3.3	Laboratory analysis	61
3.4	Calculus	67
3.5	Results	69
3.6	Results discussion	71
4	Forest carbon inventory	73
4.1	Introduction	73
4.2	Parcels settings	73
4.3	Aboveground compartment	75
4.4	Root compartment	79
4.5	Litter compartment	80
4.6	Necromass compartment	82
4.7	Total biomass carbon	85
4.8	Result discussion	87
5	Net carbon emission	88
5.1	Results	88
5.2	Result discussion	89
6	Conclusions	90
	Bibliography	92

Chapter 1

Context

1.1 Introduction

The United Nations Framework Convention on Climate Change (UNFCCC) established an international environmental treaty to combat "dangerous human interference with the climate system", in part by stabilizing greenhouse gas concentrations in the atmosphere.

The Paris Agreement was signed in 2015 and its main objective is to limit the temperature increase to 1.5 °C above pre-industrial levels. The agreement works on a 5-year cycle of increasingly ambitious climate action carried out by countries. In 2020, nations have submitted their plans for climate action known as Nationally determined contributions (NDCs). In their NDCs, countries illustrate actions they will take to reduce their Greenhouse Gas emissions to reach the Paris Agreement goals.

The 2015 Brazilian NDC establishes that Brazil must reduce its emissions by 37% by 2025 and 43% by 2030, in relation to 2005 levels. In addition, in 2021, Brazil even committed to expanding its ambition to 50% reduction by 2030 and achieving net neutral emissions by 2050, that is, everything the country emits must be compensated with sources of carbon capture, such as forest planting, recovery of biomes or other technologies.

Both developed and emerging countries agree that forests play a key role in reducing global GHGs emissions.

The world's forests have important effects on atmospheric CO_2 levels, and it's estimated that 107 Teratonnes of carbon are stored in total forest biomass and soil together (*Global Forest Resources Assessment (FRA) 2020*) which is more than the amount present in the atmosphere. The Food and Agriculture Organization (FAO) points out that the amount of atmospheric carbon transformed into forest biomass is 25-30 Gt/year.

Despite the awareness of the important role of forests, recognition of their ability to mitigate climate change is still poorly measured and gaps in knowledge are present. Additionally, maintaining biodiversity in forests contributes to their resilience, adaptive capacity, and ecosystem services, which reduce society's vulnerability to climate change (Sartori 2018). In this sense, the Atlantic forest and its inhabitants, particularly indigenous peoples, are vulnerable to the climate crisis and to disasters that can shock the region.

This means it is an important challenge for the country, at all levels of government, to create a culture of eco-sustainable practices that are supported from the grassroots and financially sustainable, using adequate funding mechanisms within the context of a participatory and results-based management approach.

The goal of this study is to present, for the Atlantic forest biome, operational procedures, results and comparison of the carbon sequestration capacity with respect to land use transformations. In order to accomplish this, different stands are considered, one still covered by the native forest (NAT), one under natural regeneration (REG) and the last devoted to cultivation of Pupunha (PUP).

The Net emissions of the regenerating forest and of the agricultural field are evaluated in relation to the unaltered forest, and computed based on the contributions of the following carbon inputs/outputs:

- greenhouse gases emitted by soil, represented by N_2O and CH_4 fluxes (computed in Chapter 2);
- soil, represented by ΔSOC (computed in Chapter 3);
- vegetation, represented by ΔTB (computed in Chapter 4).

Chapter 5 provides the net calculation of the carbon emissions/intakes derived in the aforementioned Chapters.

The hypothesis is that different land-use stands will give decreasing carbon capture values in relation to greater anthropization.

The present study is carried out under the auspices of the Brazilian Agricultural Research Corporation (Embrapa in Portuguese, Empresa Brasileira de Pesquisa Agropecuária), which is a state-owned research corporation affiliated with the Brazilian Ministry of Agriculture.

Since 1973, it has developed technologies, knowledge, and technical-scientific information for Brazilian agriculture, including livestock. A total of 63 centres comprise Embrapa's organizational structure, which includes Research units, Service units, and Central units. Such research centres are distributed throughout the country in nearly all Brazilian states, with over 9,790 employees, 2,444 of whom are researchers. In terms of international cooperation, Embrapa has bilateral agreements for technical cooperation with a number of countries and institutions, and multilateral agreements with international organizations, especially regarding joint research activities.

This research, under the guidance of Embrapa Forestry, was also made possible by 'Boticário Group Foundation for Nature Protection', through Salto Morato Natural Reserve (SMNR), which provided the data (e.g Guapyassú and Gatti 2011), the permits, the housing solutions necessary for the measurement campaigns and, most importantly, provided the opportunity to analyze data from native forests that would perhaps cease to exist without their protection.

1.2 Research site

Forest domain

Brazil can be considered a forest country, with approximately 5 million Km^2 of forests (59.4%), which represents the second largest forest area after Russia (*Global Forest Resources Assessment (FRA) 2020*).

Brazil's Atlantic Forest stretches from Rio Grande do Norte in the north to Rio Grande do Sul in the south. Inland, it extends to eastern Paraguay and the province of Misiones in northeastern Argentina, and narrowly along the coast, it reaches Uruguay. This hotspot also includes the offshore archipelago of Fernando de Noronha and several other islands off the Brazilian coast.

Long isolated from other South American tropical forests by the surrounding savannas and woodlands, the Atlantic Forest has an extremely diverse and unique mix of vegetation and forest types, making it an important world biodiversity resource. The study area is part of the alluvial Atlantic rain forest (H. P. Veloso et al. 1991), in the special usage zone of the Salto Morato Natural Reserve, in Guaraqueçaba county, north coast of Paraná State, Southern Region of Brazil; Geographic coordinates 25°11' South of Equator and 48°18' West of Greenwich Meridian. The designation "ombrophilous", of Greek origin, means "friend of the rains", because it is characterized by high rainfall well distributed throughout the year, along with relatively high temperatures, which enhance its shoulder-thermal characteristics (Fundação Instituto Brasileiro de Geografia e Estatística 1992).

The formations of the Atlantic Forest cover the area in submontane, montane, and alluvial variations. The existing formations in the Reserve are defined according to their physiognomic characteristics and altitudinal and edaphic conditions, and can be framed in the Submontane Dense Ombrophilous Forest sub-formation and divided into 4 successional phases: common capoeira, capoeira with the predominance of Asteraceae, capoeirão and forest primary.

In figure 1.1 a glimpse of the Atlantic forest of the examined site.

Protection contest

The Atlantic Forest, which once occupied a continuous coastal strip, is now sparsely distributed. The largest remnant of this formation is located in the municipality of Guaraqueçaba, which, together with the one on the southern coast of São Paulo, forms the largest continuous strip of Atlantic Forest in Brazil. This statement is corroborated by the presence of several conservation units such as the Federal and State Environmental Protection Areas of Guaraqueçaba, the Superagüi National Park, the Ecological Station of Guaraqueçaba, Pinheiro and Pinheirinho Islands and the Salto Morato Natural Reserve itself, which was recently designated a World



Figure 1.1: Salto Morato Natural Reserve

Heritage Site by UNESCO. A geographical overview of the case study site is shown in figure 1.2.

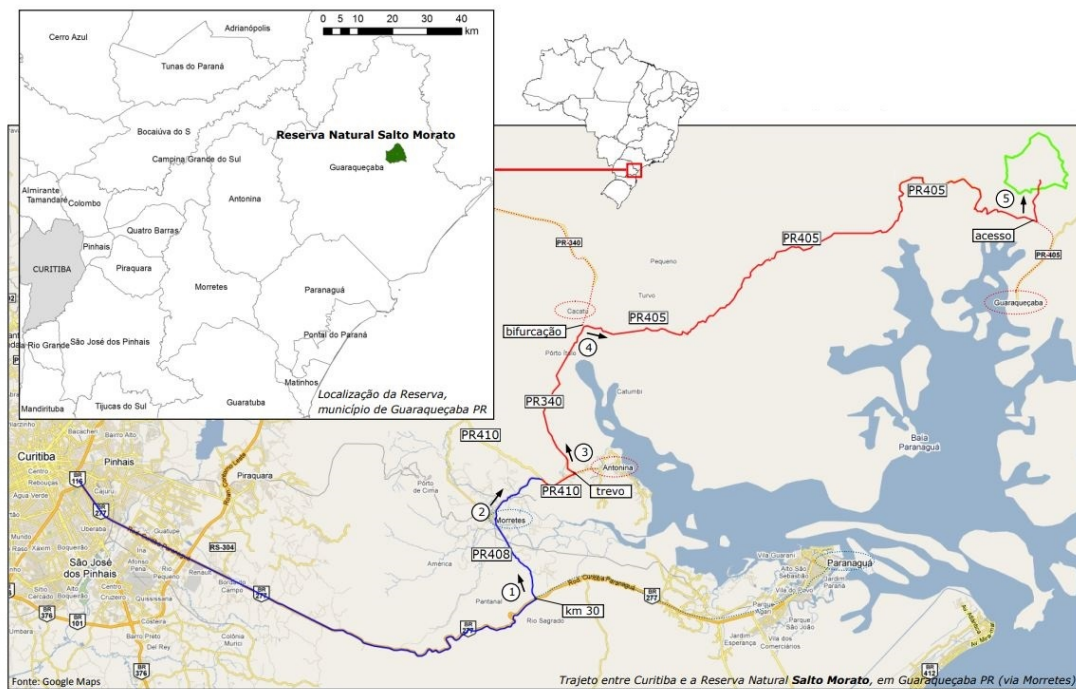


Figure 1.2: Salto Morato Natural Reserve geographical framing

The O Boticário Foundation for Nature Protection was created in 1990 by the cosmetics industry O Boticário. Among its Protected Natural Areas program, the Salto Morato Natural Reserve opened in February 1996, with the goal of preserving and perpetuating an important stretch of Atlantic Forest. As a private reserve of natural heritage, the SMNR is managed in accordance with the precepts of a national park. As a result, it is geared toward preserving nature, protecting scenic beauty, encouraging scientific research and environmental education, and contributing to environmental monitoring.

Climate

Literature values indicate an average daily temperature of 18 °C during the coldest month and 22 °C during the warmest month, with hot and wet summers (January-March) and a less pronounced dry season; the mean annual rainfall is 2,403mm (Scheer 2008).

During the 2018-2022 timeframe, data analysis has been performed on the Simepar (Paraná Environmental Technology and Monitoring System) weather station installed in the study area. The mean temperature and rainfall in 24h for the warmest and coldest months are shown in table 1.1; the mean annual rainfall has been 2447 mm.

2018-2020	Mean T [°C]	Mean rainfall 24h [mm]
January	25.61	13.63
July	16.97	1.28

Table 1.1: SMNR Simepar weather station data

The climate of the region is classified as subtropical or transitional tropical. According to Koppen's climate classification map (figure 1.3), Parana's coastline is classified as Cfa (humid - oceanic climate - with hot summer). Figure 1.4 reports these specifics.

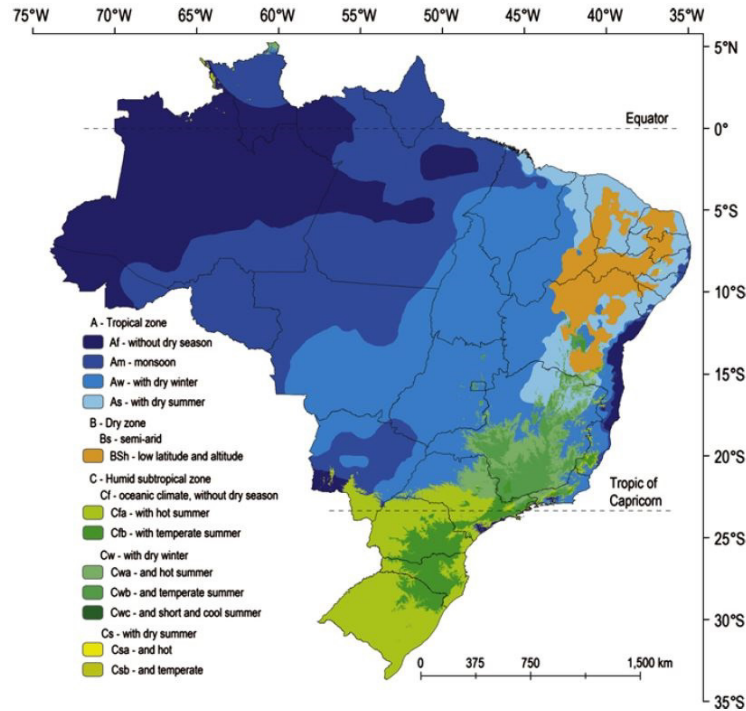


Figure 1.3: Brazil Koppen's climate classification

Temperature		Rainfall		Climate		Symbol	
T _{COLD}	T _{HOT}	T _{ANN}	R _M	R _{ANN}			
≥ 18 °C			R _{DRY} ≥ 60 mm R _{DRY} < 60 mm	≥ 25 (100 - R _{DRY}) < 25 (100 - R _{SDRY}) < 25 (100 - R _{WDRY})	(A) Tropical	(f) without dry season (m) monsoon (s) with dry summer (w) with dry winter	Af Am As Aw
		≥ 18 °C < 18 °C ≥ 18 °C < 18 °C		≥ 5 * R _{THRESHOLD} < 10 * R _{THRESHOLD} < 5 * R _{THRESHOLD}	(B) Dry (S) Semi-arid (W) Arid	(h) low latitude and altitude (k) mid-latitude and high altitude (h) low latitude and altitude (k) mid-latitude and high altitude	BSh BSk BWh BWk
≥ -3 °C & < 18 °C	≥ 22 °C	≥ 22 °C & T _{M10} ≥ 4 < 22 °C & 1 ≤ T _{M10} < 4	R _{DRY} > 40 mm	R _{DRY} < 40 mm R _{SWET} ≥ 10 * R _{WDRY}	(C) Humid subtropical	(f) Oceanic climate, without dry season (a) with hot summer (b) with temperate summer (c) with short and cool summer	Cfa Cfb Cfc
≥ -3 °C & < 18 °C	≥ 22 °C	≥ 22 °C & T _{M10} ≥ 4		R _{DRY} < 40 mm R _{SWET} ≥ 10 * R _{WDRY}		(w) With dry winter (b) and temperate summer (c) and short and cool summer	Cwa Cwb Cwc
≥ -3 °C & < 18 °C	≥ 22 °C	≥ 22 °C & T _{M10} ≥ 4		R _{DRY} < 40 mm R _{WWET} ≥ 3 * R _{SDRY}		(s) With dry summer (a) and hot (b) and temperate	Csa Csb
≥ -3 °C & < 18 °C	≥ 22 °C	≥ 22 °C & 1 ≤ T _{M10} < 4		R _{SWET} < 10 * R _{WDRY} R _{DRY} > 40 mm	(D) Temperate continental	(f) Without dry season (a) with hot summer (b) with temperate summer (c) with short and cool summer	Dfa Dfb Dfc
≥ -3 °C & < 18 °C	≥ 22 °C	≥ 22 °C & T _{M10} ≥ 4		R _{DRY} < 40 mm R _{SWET} ≥ 10 * R _{WDRY}		(d) with very cold winter (a) with hot summer (b) and temperate summer	Dfd Dwa Dwb
≥ -3 °C & < 18 °C	≥ 22 °C	≥ 22 °C & 1 ≤ T _{M10} < 4		R _{DRY} < 40 mm R _{SWET} ≥ 10 * R _{WDRY}		(w) With dry winter (b) and temperate summer (c) and short and cool summer	Dwb Dwc
≥ -3 °C & < 18 °C	≥ 22 °C	≥ 22 °C & T _{M10} ≥ 4		R _{DRY} < 40 mm R _{WWET} ≥ 3 * R _{SDRY}		(s) With dry summer (a) and hot (b) and temperate	Dwd Dsa Dsb
≥ -3 °C & < 18 °C	≥ 22 °C	≥ 22 °C & 1 ≤ T _{M10} < 4		R _{SWET} < 10 * R _{WDRY}		(c) and short and cool summer (d) and very cold winter	Dsc Dsd
< -38 °C & < -3 °C	< 10 °C & ≥ 0 °C	< 0 °C			(E) Polar	(T) Tundra (F) Frost	ET EF

C. A. Alvares et al.: Koppen's climate classification map for Brazil

T_{COLD} = Temperature of the coldest month; T_{HOT} = Temperature of the hottest month; T_{ANN} = Annual mean temperature; R_M = Monthly Rainfall; R_{ANN} = Annual Rainfall; R_{DRY} = Rainfall of the driest month; R_{SDRY} = Rainfall of the driest month in summer; R_{WDRY} = Rainfall in the driest month in winter; R_{SWET} = Rainfall of the wettest month in summer; R_{WWET} = Rainfall in the wettest month in winter; T_{M10} = number of months where the temperature is above 10 °C; R_{THRESHOLD} = varies according to equation 1; For the southern hemisphere summer is defined as the warmer six month period (ONDJFM) and winter is defined as the cooler six month period (AMJJAS). For the northern hemisphere summer is defined as the warmest six month period (AMJJAS) and winter is defined as the coolest six month period (ONDJFM).

Figure 1.4: Koppen's classification specifics

This classification is confirmed by 2018-2022 data from the site weather station, which provides the following values:

T cold [°C]	T hot [°C]	R dry [mm]
26	17	40

Table 1.2: SMNR Simepar weather station data

Geology

Four geological environments occur in SMNR: a pre-setuva complex, a migmatite complex, anatexia granitic suite, and recent sediments; lower and upper proterozoic rocks are found there.

These soils originate from the Cenozoic sediments of Serra do Morato (uplifted blocks of igneous and metamorphic rocks) and are primarily medium-textured Fluvisols and Cambisols. Clay content ranges from 35 - 60% in the soil texture. Fertility is poor in the region due to a lack of the main nutrients.

In assessing the geomorphological characterization, three different units are considered: the mountain range, the colluvial area, and the plain.

Geotechnical factors confer high risk to about 80% of the area. The expected phenomena arising are laminar erosion/furrows, landslides, slippage, block rolling, rock displacement, flooding, riverside erosion, silting, and others.

The altimetry of the site is depicted in figure 1.5.

Hydrology

In the 2011 Reserve Management Plan, the rock substrate geodiversity suggests two types of aquifers may exist: crystalline aquifer (fractured or fissured) and porous (alluvial) aquifer.

Crystalline aquifers occur in association with crystalline rocks (migmatites, gneisses, granitoids, and schists) and their water accumulation and circulation are related to the number of fractures, openings, and connections. There is a reasonable hydrogeological potential for the SMNR rocks due to their brittle structural weave. A surplus of saturated zone in the southeastern part of the Reserve causes the water table to rise, forming ponds.

Porous aquifers, on the other hand, are associated with unconsolidated sediments present in the valley bottom and floodplain areas, where sandy sediments have accumulated.

The recharge method is directly related to rain, which saturates the alluvial bed, also through lateral surface runoff.

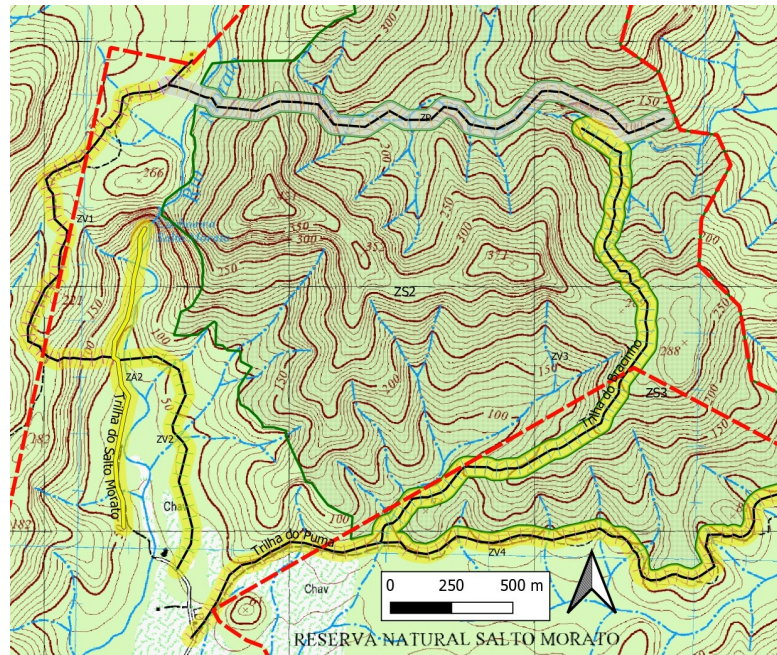


Figure 1.5: Salto Morato Natural Reserve topographic map

Biotic factors

Brazil's Atlantic Forest ranks among the world's top five biodiversity hotspots, yet it is also among the rainforests most affected by human activity. Despite the anthropization, over 20,000 plant species can be found, including 8,000 endemic species; there are also 261 mammals (of which 73 are endemic), 620 birds (160 endemic), and 260 amphibians (128 endemic).

Criticalities

Livestock activity in Guaraqueçaba region results in deforestation in large areas, erosion, and a drop in water quality due to inadequate management. Lowland forests are frequently cleared to make way for buffalo farms. In addition, the hillside forests were cleared of hardwood trees of commercial interest or for local use, and even in areas with a greater declivity, banana plantations or subsistence agriculture replaced the forest.



Figure 1.7: Natural forest aspect

It occupies 481.8 ha, corresponding to 21.4% of SMNR domain. Figure 1.7 shows its outlook.

Regenerated forest

The region occupies around 1,096 hectares and has been significantly altered by humans directly or indirectly.

It includes areas in various stages of succession, as well as stagnant succession spots. Recovery measures can be adopted if restoration encounters obstacles, such as densifying native species or removing exotic invasive species on a continuous basis. However, this study only analyzes areas where natural restoration is taking place, such as in figure 1.8.

In detail, these portions are part of a natural secondary succession process that began 29 years ago after buffalo breeding was abandoned. The original lush forest was instead cleared many decades ago, but the date of this clearcut is uncertain; according to a resident report, the forest had already been cut down in the 1950s, but there is not enough evidence to say if it was a primary formation or an advanced secondary forest. After the felling, the area was used for subsistence purposes and small trade and sales of white crops including maize, beans, rice and sweet



Figure 1.8: Regenerated forest aspect

potatoes. Following this period of subsistence farming, the area started to be used for banana cultivation in 1983. In this phase the field was mowed and crowned, usually without using fires, chemical products, or hoes. In 1988, buffalo pasture was established in this area. The banana plantation was destroyed by buffalos that trampled the soil and ate the plants. For animal feed, *Brachiaria* (signalgrass) was planted, primarily humidicola brachiaria, which grows well on moist soils. In 1994, after the purchase by 'O Boticário Foundation', buffalo farming was abolished and the 560'000 m^2 of pasture (dotted in figure 1.9), were destined for natural restoration.

Forest succession progress

2010 The areas chosen for restoration were still in the early stages of succession, with a significantly higher dominance of grasses than woody species and with a low density of arboreal plants, which are predominantly early pioneers.

2017 The restoration process appears to be progressing satisfactorily and the resilience of the ecosystem is discovered not to be compromised by the anthropogenic changes suffered. A visual analysis confirmed the recovery of tree and shrub components to the detriment of herbaceous vegetation.

SMNR's Succession Project 2017 reports the following data:

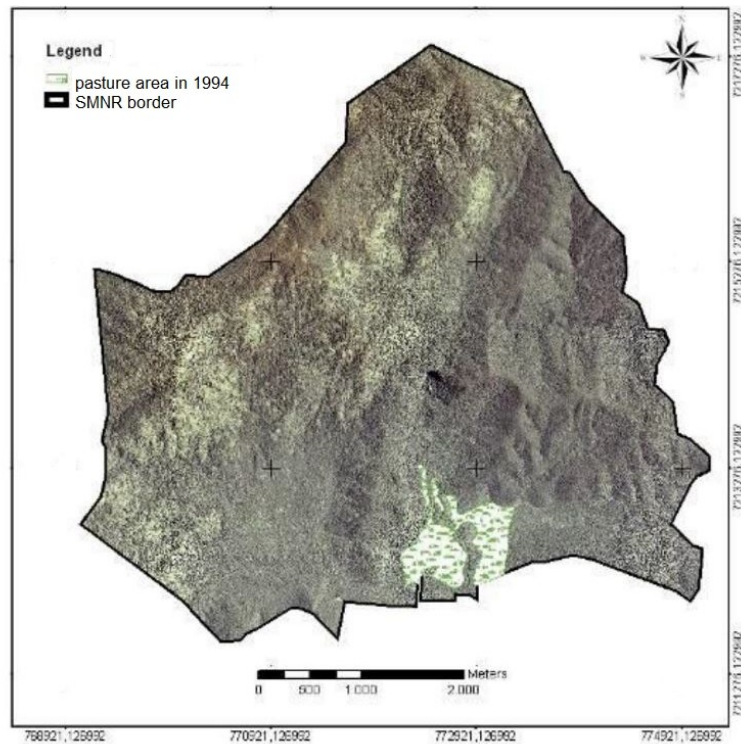


Figure 1.9: Pasture area in 1988-1994

- species richness (S) → 85% of which 15% shrubs and 85% arboreal;
- density (N/ha) → 2700 of which 800 bushes and 1900 trees;
- basal area (m^2/ha) → 29 of which 4 bushes and 25 tree.

Pupunha culture

Prior to being a culture, this area also served as buffalo pasture for more than 20 years. In 2018, it began cultivating *Bactris gasipaes* (Peach palm), which is grown, in this case, to produce palm hearts (figure 1.10).

This species has several advantages: the ability to regrow, the product in nature doesn't oxidize, and production begins 18 months after planting and continues for 15 years, with annual harvests. Plantation of peach palms for palm hearts sale is recognized by the FAO as a good practice, and by the Banco do Brasil Foundation as a social technology. Replacing a pasture area, which in the case of buffalo farming consists of grasses, with peach palm which consists of shrubs, leads to environmental gains also in terms of carbon sequestration.

The property belongs to an employee of SMNR, Mr Lino, who generously permitted us to take the measurements.



Figure 1.10: Pupunha culture aspect

1.4 Parcels configuration

Parcels intensity

Sampling intensity is determined by parameter population variability. A large variance will result in high sampling intensity and high sampling costs. Carbon stock can be quantified at an acceptable cost with a sampling error of 10% over the mean value at 95% confidence level, while errors up to 20% can be accommodated (Pearson et al. 2005).

According to some characteristics such as topography, geology, hydrology, anthropization degree, physiognomy, forest typology, tree height, age, species density, and others, heterogeneous populations are usually divided into subpopulations/homogenous strata. However, stratification is based on the principle that even when variation in other compartments is greater, if high precision is achieved in the dominant compartment, a loss of precision in others will not detract from the results overall. Based on the variance of the major carbon source, the aerial biomass in this case, the intensities reported in the dedicated chapters capture the majority of the variance.

Parcels distribution

Sampling involves the preliminary allocation of sampling plot locations. In general, native forest areas cannot be quantified using conglomerates because they are discontinuous and often narrow. Therefore, the Stratified random measuring method is considered to be the most appropriate, where parcels are allocated randomly within homogeneous strata. The distinct parameters input ports can also be arranged arbitrarily within each parcel since it is randomly allocated within

congruent strata.

In the case of chronosequences in land use, special attention must be given to the selection of sites with similar soil and granulometric composition. This claim has been supported by soil tests. The tests refer to visual comparison of clay content and to chemical and granulometric analyzes, these being carried out in different environments (various altitudes, vegetation cover, hydrological conditions, etc.). The tests led to characterize the soils as homogeneous for the required level of precision, and therefore to confirm a random distribution of the measurement plots and an effective comparison between stands.

1.5 Definitions

The terminology used in the following chapters is outlined here.

Forest

A minimum of 0.05 to 0.1 ha, with a canopy coverage of at least 10% to 30%, and trees capable of reaching at least 2m to 5m in height when mature (Eggleston 2006);.

Biomass

Total amount of organic matter, dead or alive, both above and below ground, existing in organisms, animals or plants, in a given community. It is expressed as dry matter mass (DM) per unit area. The biomass amount depends primarily on age, soil type, climate conditions and use history.

According to Birdsey et al. 2006, its measurement implies the quantification of four carbon reservoirs: aboveground biomass, belowground biomass (roots), litter and necromass (figure 1.11).

Aboveground biomass

Includes trunks, stumps, branches, crowns, seeds, and leaves.

Root biomass

Defined as living or dead underground biomass over 2 mm in diameter.

Litter

Plant material (leaves, flowers, thin twigs, bark, fruits, seeds) and, to a lesser extent, animal material (animal remains and fecal material) deposited on the soil surface. Material less than 2 cm in diameter, in different stages of decomposition, is sampled within this group.

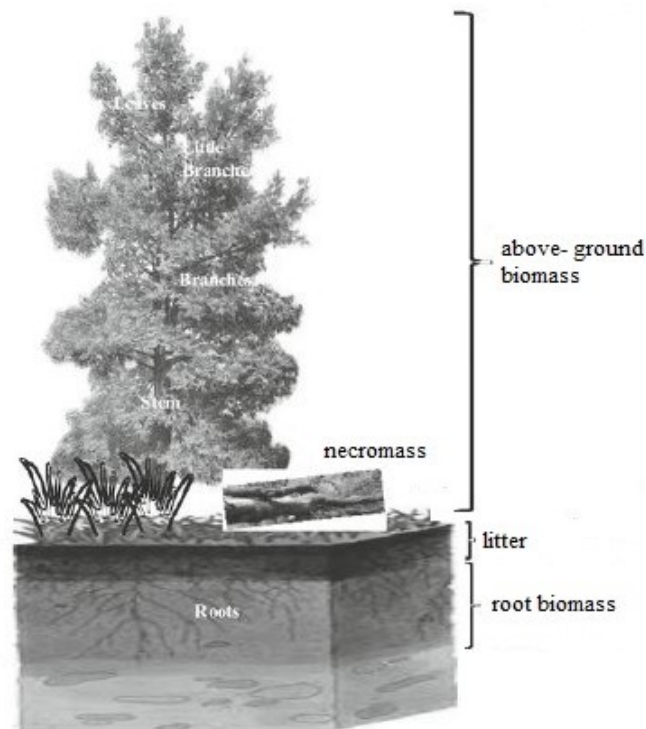


Figure 1.11: Forest biomass partition

Necromass

Refers to woody material found on the forest floor, including logs, twigs, wood fragments, branches and roots. The diameter should be at least 2 cm.

Carbon

SOM - Soil organic matter

It's composed mainly of carbon, hydrogen and oxygen, and small amounts of other elements, such as nitrogen, phosphorous, sulfur, potassium, calcium and magnesium contained in organic residues. It can be divided into living and dead substances, ranging from recent materials, such as stubble, to long-decayed ones.

SOC - Soil organic carbon

It's a measurable component of SOM. Soil organic matter is just 2–10% of soil mass and plays a vital role in physical, chemical, and biological processes.

Carbon stock

It refers to the quantification of the carbon mass found in forest biomass.

Typically, this element represents 47% of the dry mass of the total biomass and is stored in different compartments.

ETC - Ecosystem total carbon

It's the sum of SOC, tree carbon, litter and necromass stocks.

1.6 Carbon balance

Three inputs and outputs are taken into consideration when quantifying the carbon stored in the Atlantic forest: the GHGs emission from soil, the amount in forest biomass, and the amount in soil; expressed as *CO₂ equivalent*.

Chapter 2

Greenhouse gases emissions

2.1 Introduction

Gas collection chambers are exploited, which accumulate gases within an open-bottomed chamber placed on the soil surface. Samples are collected with syringes and then transferred to evacuated vials for transport and storage until analysis. Finally, the concentrations of some key GHGs are determined by chromatography. Flux measurements from a given number of chambers, over a stated time period and with a specified sampling frequency, are executed to determine spatially and temporally integrated emissions. The procedure will evaluate the flux of methane (CH_4), nitrous oxide (N_2O) and carbon dioxide (CO_2) from the soil. However, CO_2 emissions are not measured for the purpose of calculating GHGs fluxes, since part of the emission comes from roots respiration and decomposition of soil organic matter. CO_2 is estimated for verification purposes only because it shows significant outliers in case of errors.

As with all other techniques, the chamber methodology can bias results or bias third-party interpretations. The international science community recognizes the need for standard guidelines on the use of chambers, associated data reporting and data analysis. These are discussed in Klein and Harvey 2015, and adopted in this dissertation.

2.2 Sampling

Instrumentation

Static chambers, specifically non-flow-through non-steady-state (NSS) chambers, have been the most widely used method for measuring gas fluxes from agricultural

soils for the past 30 years; Embrapa adopted them based on the positive experience gained so far. Furthermore, closed static chambers are also more economical than semi-automatic or automatic chambers, allowing more points to be evaluated. Chambers of this type consist of two parts: the base and the top (figure 2.1).



Figure 2.1: Chamber configuration

The base is a circular steel support embedded in the ground that contains a channel on which the top of the chamber is placed (figure 2.2). In order to avoid obstructing air circulation or accumulating water inside the base, the height of the channel does not exceed 5 cm. With its dimensions compatible with the top, the channel offers a perfect seal that is reinforced by a rubber ring placed on the lower part of the chamber body.

Measurements should avoid plants being present, and if necessary, these need to be uprooted; this is because plants can significantly affect N_2O fluxes.

The top of the chamber, which is trivially a 30L plastic bucket, incorporates a thermometer, a fan and a sampling valve (figure 2.3).

The fan is a 12 V computer cooler. In a chamber with no constant mixing of gas during the enclosure period, soil gas fluxes can be underestimated (Liu and Si 2009); thus, the fan is provided to overcome possible bias from vertical gas concentration gradients. An external battery is required to activate the fan, which is transported by the collector during collection.

The sampling valve is a three-way “luer lock” outlet type. Furthermore, a polyurethane pipe extension is installed so that the sample is taken 20-30 cm

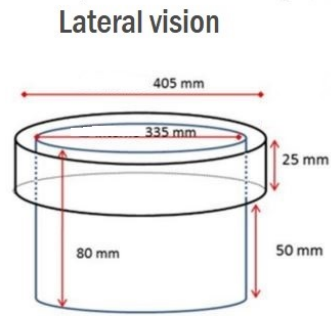


Figure 2.2: Chamber base



Figure 2.3: Chamber toolkit

above ground level in the center of the chamber.

A skewer thermometer is used.

The body chamber is covered with an aluminized blanket to avoid large differences in internal and external temperature.

The format and materials ensure non-reactivity, easy production, comfortable handling, low cost, as well as meeting technical specifications.

The production budget is around 45€ (220R\$) per camera.

Sampling intensity

The GHGs measurement design includes three parcels of four chambers each, for each forest configuration (NAT/REG/PUP). Four samples at different times are collected from each of the 12 chambers, leading to a total of 48 syringes for each forest stand.

Based on a previous study in Santa Catarina, 350 km from SMNR, 9 chambers/600 m^2 were determined to be the minimum number of evaluation points.

A total of four collections are taken during each chamber's incubation period. The time scan most often used is 0, 20, 40, 60 minutes; however, some slightly different intervals have been sometimes adopted due to logistical needs in the distribution of the instrumentation.

Concentrations at different times have been previously verified to be linear; if the final concentration remains linear with the recorded times, this indicates that the increase in gas concentration inside the chamber has no suppressive effect on the gas diffusion inside the soil. Anyhow the total incubation time should be as short as possible, as long as it is sufficient for the accumulation or reduction of gas to be observed. The scans adopted are in line with Serta 2013, which recommends a final time greater than 40 minutes, but not more than 120 minutes.

Regarding the frequency of field campaigns, as for forest systems the "crop" dynamics are slow, long time intervals between collections can be adopted.

This report also incorporates data from GHGs measurements conducted prior to those in which I participated. This ensures more accurate and representative outcomes as, starting from 22/06/2021 to 19/05/2022, different seasons are accounted, which are known to influence emissions.

It should be pointed out that, due to the restrictions for the containment of the COVID-19 pandemic, it was not always possible to detect at the set frequency; however the representativeness of seasons is guaranteed.

The variations resulting from different weather conditions are also accounted for by sampling under different climate circumstances.

Finally, since diurnal temperature variations affect gas concentrations, the collections are conducted at mid-morning, a time that better coincides with daily average temperature.

Parcels location

GPS UTM (Universal Transverse Mercator) coordinates are used to pin the locations.

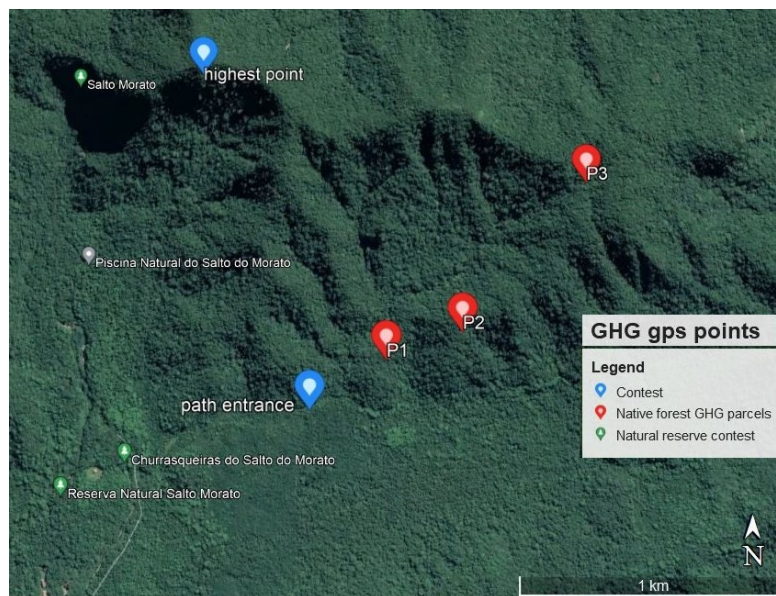


Figure 2.4: Native forest GHGs measuring points

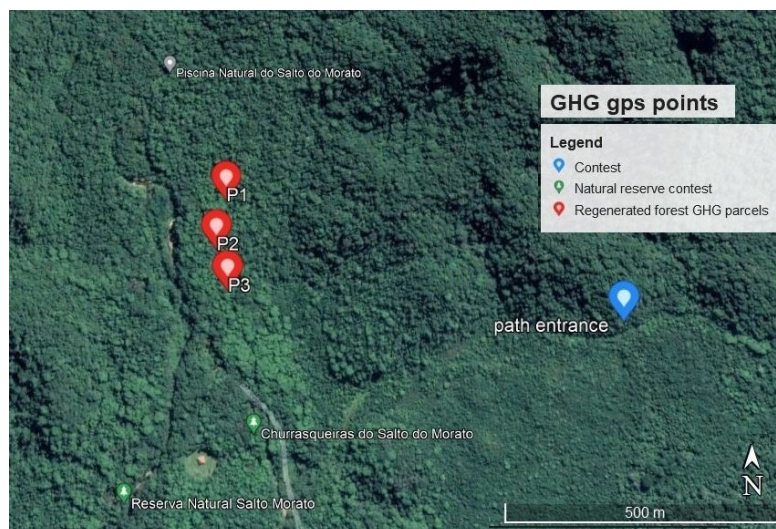


Figure 2.5: Regenerated forest GHGs measuring points



Figure 2.6: Pupunha culture GHGs measuring points

Sampling steps

Step 1: Turn on the thermometer and open the sampling valve to allow internal pressure outlet.

Step 2: Place the chamber body over the base. Close the valve immediately and start the timer.

Step 3: Connect the syringe n°1 to the valve and pump the plunger five times to withdraw the t_0 air sample. Remove the syringe and store it in a cooler.

Step 4: Record the temperature inside the chamber in the field spreadsheet, along with any other observations.

Step 5: Wait the necessary time to collect t_1 sample (e.g. chronometer time = 20 min). At 30 seconds before t_1 , turn on the fan; at collection, turn it off and proceed according to steps 3 and 4.

Step 6: Repeat step 5 but with t_2 sample (e.g. 40 min).

Step 7: Repeat step 5 but with t_3 sample (e.g. 60 min).

Step 8: End of collection. Remove the chamber from the base by previously opening the valve, this prevents the internal pressure from making it difficult to pull it.

To facilitate the understanding, the steps reported above relate to the acquisition by one team member working on one chamber at a time. In practice, however, one person collects from several chambers at the same time. Note that the timer is only activated once, at the beginning of the collection.

The temperatures inside the chambers are likewise reported in the field spreadsheet for each collection time.

Finally the actual procedure is:

Step 1: The operator starts from chamber n° 1, activates the stopwatch and collects the t_0 air sample.

Step 2: At 2'00" from the timer start, the same person collects the t_0 sample from chamber n° 2, in 4 minutes the one from chamber n° 3, etc.

Step 3: At 19'30", the collector returns to chamber n° 1 and turns on the fan for 30 seconds.

Step 4: At 20'00", the fan is turned off and the t_1 air sample is collected from chamber n° 1.

Step 5: Then the team member moves to the other chambers, always in intervals of 2 minutes, and repeats the procedure until the end of each chamber's collection time.

Figure 2.7 illustrates an example of the spreadsheets used on field campaigns.

Samples handling

The gas samples collected in the 20 mL polypropylene syringes are transferred, in a range of 1-2 hours after collection, into evacuated 12 mL vials by means of a needle (figure 2.8).

Greenhouse gases emissions

Coleta Guaraqueçaba							
COLETA Nº 17							
Pasto/Pupunha							
Estação:	Verão			Horário início: 8:10			
Data:							
Coletor:	Claudia		Rosanna				
Tempo:	suel						
Parcela	Nº Base	Tempo (min)	Nº Seringa	Nº frasco	Temperatura Câmara (°C)	Temperatura Solo (°C)	Observações
P1	1	0	97	6548	24.4		
		24	98	6549	32.1		
		48	99	6550	32.7	23.4	
		72	100	6551	41.8		
	2	2	101	6552	25.6		
		26	102	6553	27.2	23.3	
		50	103	6554	29.2		
		74	104	6555	31.3		
	3	4	105	6556	24.2		
		28	106	6557	21.2	23.4	
		52	107	6558	24.4		
		76	108	6559	21.7		
4	6	109	6560	26.3			
	30	110	6561	27.8	23.5		
	54	111	6562	30.3			
	78	112	6563	31.1			
P2	5	8	113	6564	25.9		
		32	114	6565	30.4	23.7	
		56	115	6566	31.2		
		80	116	6567	35.3		
	6	10	117	6568	24.8	23.7	
		34	118	6569	27.6		
		58	119	6570	26.5		
		82	120	6571	41.1		
	7	12	121	6572	30.3		
		36	122	6573	32.8	23.7	
		60	123	6574	34.6		
		84	124	6575	36.6		
8	14	125	6576	26.2			
	38	126	6577	29.8	23.8		
	62	127	6578	31.2			
	86	128	6579	33.3			
P3	9	16	129	6580	25.0		
		40	130	6581	35.0	23.2	
		64	131	6582	40.2		
		88	132	6583	41.3		
	10	18	133	6584	26.7		
		42	134	6585	30.9	23.8	
		66	135	6586	32.7		
		90	136	6587	33.7		
	11	20	137	6588	29.7		
		44	138	6589	37.5	23.6	
		68	139	6590	40.4		
		92	140	6591	42.1		
12	22	141	6592	26			
	46	142	6593	32.1	23.7		
	70	143	6594	35.6			
	94	144	6595	42.0			

Figure 2.7: PUP GHGs measurement field spreadsheet



Figure 2.8: Syringe and vial for GHGs

Syringes and vials require cleaning and evacuation. For campaigns with a large number of samples, a semi-automatic system is employed (figure 2.9). Furthermore, the system allows for the standardization of the flasks' vacuum, preventing differences in the dilution of samples. Cleaning and evacuation are performed in a single perforation, thereby increasing septum life.



Figure 2.9: Cleaning and evacuation system

The system basically consists of two flow paths: vacuum pressure pathway and nitrogen gas for cleaning pathway.

The operation is as follows:

Step 1: Insert the vials or syringes in the holder needles.

Step 2: Open the “vacuum-flow” and wait for total evacuation.

Step 3: Open the “ N_2 - flow” and wait for total fill.

Step 4: Repeat steps 2 and 3 twice, then step 2 again to maintain vacuum in the flasks. Without closing the “vacuum-flow”, remove the vials or syringes from the needles taking care they all come out at the same time.

2.3 Laboratory analysis



Figure 2.10: Embrapa chromatograph

The process involves the use of a chromatograph, its software and Excel for data processing.

The working principle of the employed chromatograph (figure 2.10) is the comparison of the peak area of some standard gases (of known concentration) with the peak area of samples (of unknown GHGs concentration), thus allowing to achieve the samples concentrations of CH_4 , N_2O and CO_2 .

Regarding CH_4 and CO_2 , the peak area is the product of the electric current intensity (in pA) of the signal recorded by the chromatograph and the time of occurrence of that signal (in min). For N_2O , the peak is instead the product of the frequency (in kHz) and the time of signal occurrence (in min).

The hardware is Thermo Scientific™ trace 1310. This model has a column for gases separation (divided in two channels, CH_4 - CO_2 flux and N_2O flux) and a column for prior water removal.

The software is Chromeleon™ Chromatography Data System (CDS). The interface shows the results by organizing them in 'Front detector', that is the ionization detector for CH_4 and CO_2 , and 'Back detector', that is the ECD-electron capture detector for N_2O .

To achieve the concentrations of the samples, the following procedure is followed:

Step 1: Machinery stabilization

Optimal chromatograph parameters are ensured by performing this setup, which takes at least 1 day.

Step 2: Operation-gases opening

He is used by the carrier gas, N_2 and *He* by the ECD detector and H_2 and synthetic air by the ionization detector.

Step 3: Setup of vials slots

As suggested by Timothy B. Parkin and Venterea 2010, the samples are analyzed based on collection times within each chamber (t_0 , t_1 , t_2 and t_3) to the detriment of sorting by overall acquisition time.

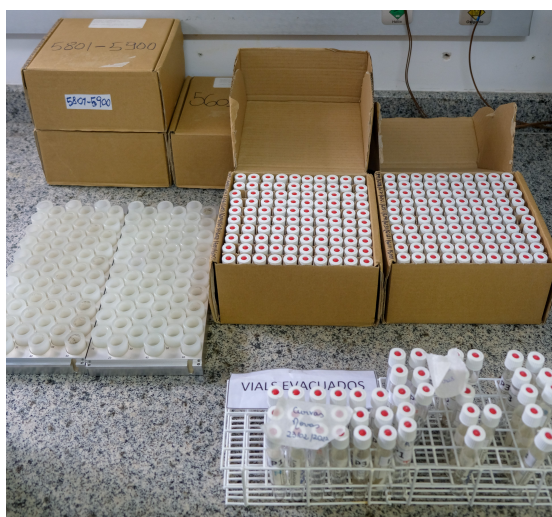


Figure 2.11: Slot filling setting

Step 4: Calibration curves

Before analyses are performed, the calibration curves are constructed. During sample analysis, check standards are periodically inserted, every 20 samples, to confirm the good performance of the equipment. Certified companies audit the standards.

The analysis now starts and for each calibration standard P_i , a curve is displayed in real-time. Note that if the basic level of the signal is not horizontal, it means

that the chromatograph is not stabilized enough.

These are the chromatograph outputs for the standard $P2$ used in the calibration curves of CH_4 (figure 2.12), N_2O (figure 2.13), and CO_2 (figure 2.14).

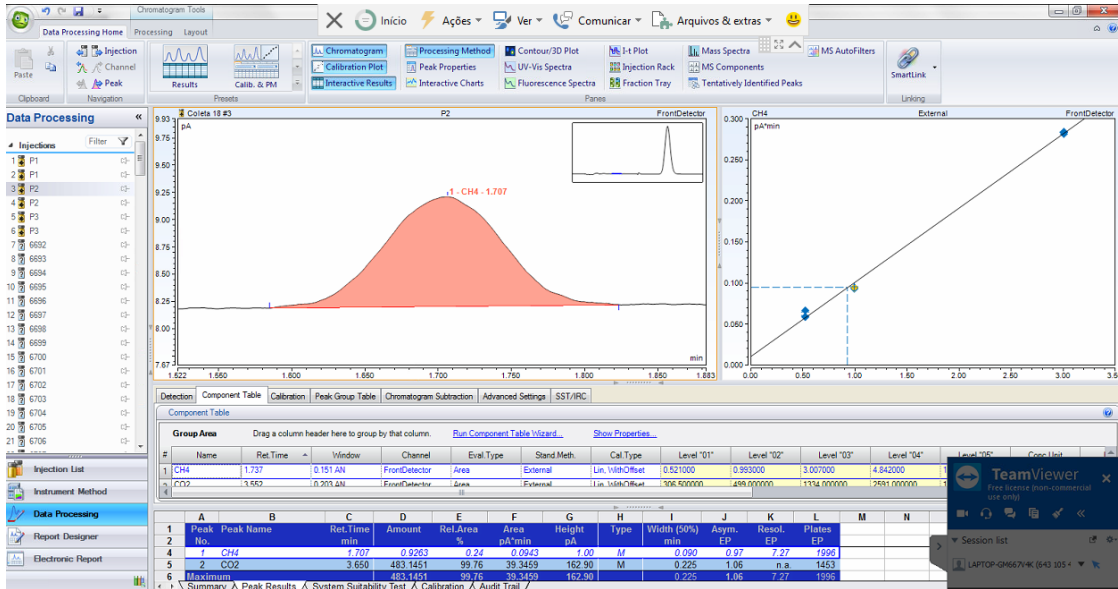


Figure 2.12: $P2$ -standard CH_4 output

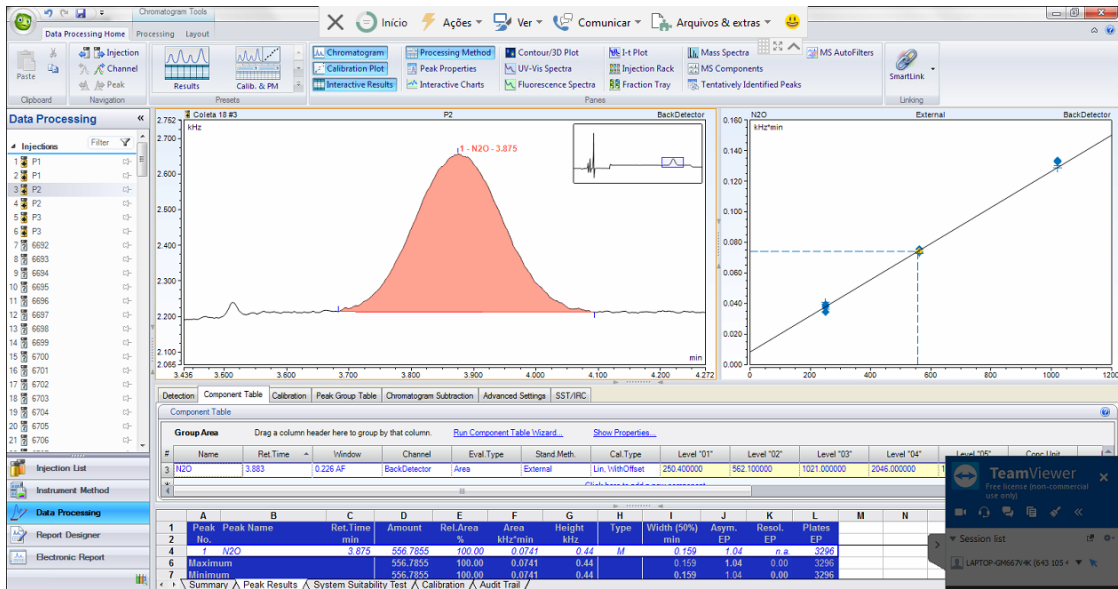
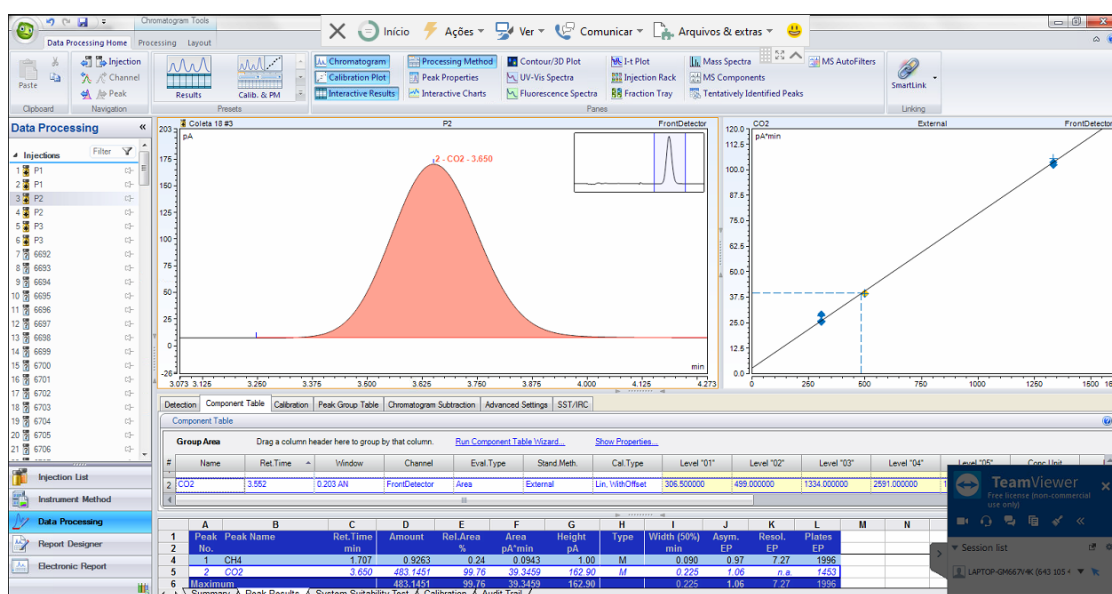


Figure 2.13: $P2$ -standard N_2O output

Figure 2.14: P2-standard CO_2 output

From the analysis of all calibration standards, usually at least 6, a straight line for each gas is computed by interpolation; the numerical values and their coefficient of determination R^2 are acquired. The following figures show the final calibration curves for CH_4 (figure 2.15), N_2O (figure 2.16) and CO_2 (figure 2.17), where the x-axis represents the known concentrations of the standards (in ppm/ppb) and the y-axis the peak areas obtained from curve integration ($pA \cdot min$ for CH_4 and CO_2 , $KHz \cdot min$ for N_2O).

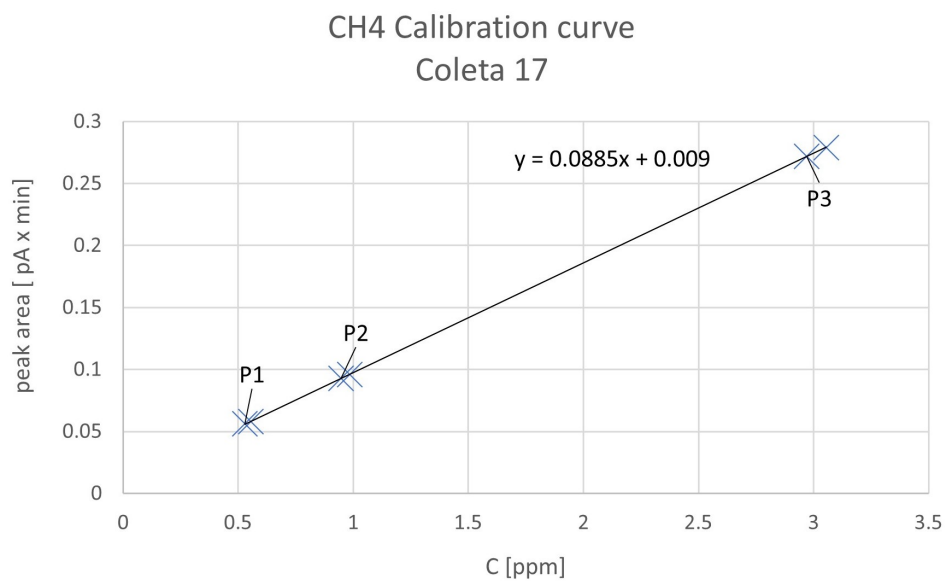


Figure 2.15: CH₄ calibration curve

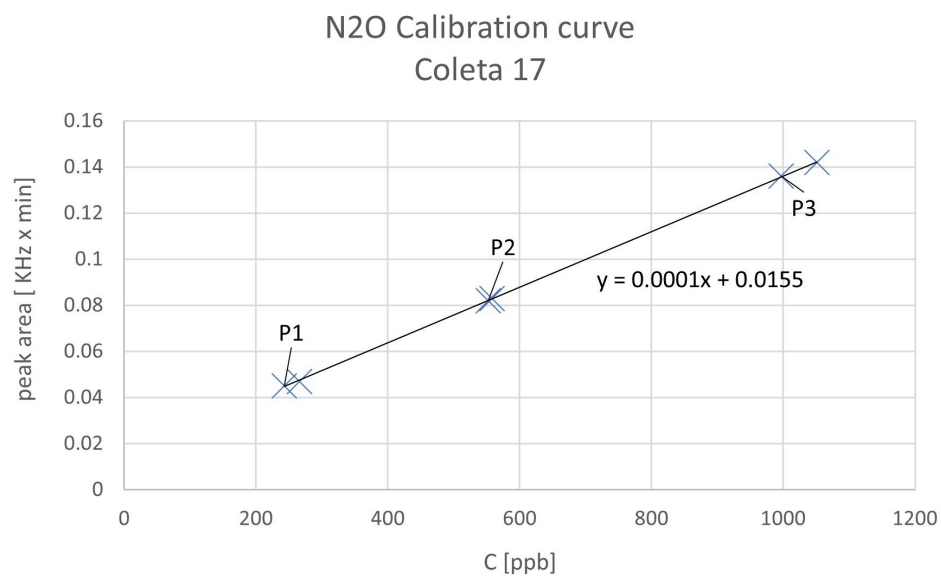


Figure 2.16: N₂O calibration curve

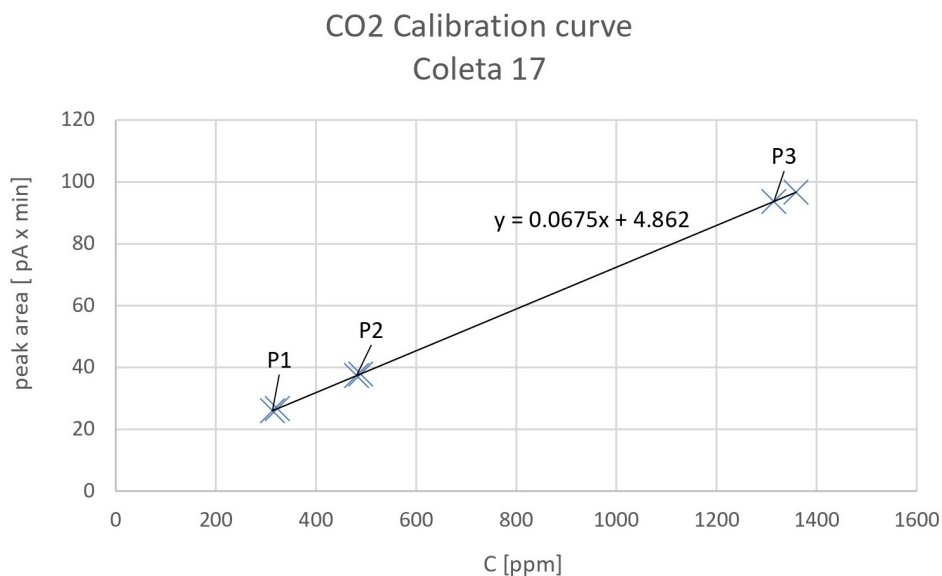


Figure 2.17: CO_2 calibration curve

By means of the straight line equation, the slope C_1 and the intercept C_0 are extrapolated:

$$\text{peak area}_{\text{standard}} = C_1 \cdot C_{\text{standard}} + C_0 \rightarrow C_1, C_0 \quad (2.1)$$

For accurate results, Step 4 should be performed every week.

Step 5: Samples concentrations

The sample peak areas are now measured by the chromatograph. From these and making use of the parameters C_1 and C_0 achieved in Step 4, the sample concentrations are automatically assessed according to the formula:

$$C_{\text{sample}} = \frac{\text{peak area}_{\text{sample}} - C_0}{C_1} \quad (2.2)$$

The results provided by the chromatograph are reported in Excel. The following tables are presented as examples of CH_4 (figure 2.18), N_2O (figure 2.19) and CO_2 (figure 2.20) concentrations of the samples.

Greenhouse gases emissions

Name:		Coleta 17			Created On:	06/Apr/22 15:06:41	
Directory:		BOTICARIO			Created By:	Embrapa Floresta GC	
Data Vault:		Embrapa_set_18			Updated On:	19/Apr/22 08:16:06	
No. of Injections:		156			Updated By:	Embrapa Floresta GC	
By Component		CH4					
No.	Injection Name	Ret.Time min	Area pA*min	Height pA	Amount	Rel.Area %	Peak Type
		FrontDetector	FrontDetector	FrontDetector	FrontDetector	FrontDetector	FrontDetector
		CH4	CH4	CH4	CH4	CH4	CH4
1	P1	1.705	0.058	0.613	0.556	0.22	M
2	P1	1.7	0.056	0.594	0.53	0.21	M
3	P2	1.7	0.093	0.991	0.947	0.25	M
4	P2	1.705	0.096	1.019	0.985	0.25	M
5	P3	1.705	0.279	2.991	3.055	0.29	M
6	P3	1.705	0.272	2.922	2.969	0.29	M
7	17_6548	1.675	0.168	1.793	1.8	0.36	M
8	17_6549	1.708	0.161	1.706	1.716	0.22	M
9	17_6550	1.708	0.159	1.67	1.692	0.17	M
10	17_6551	1.708	0.156	1.649	1.663	0.15	M
11	17_6552	1.708	0.169	1.792	1.805	0.39	M
12	17_6553	1.707	0.166	1.758	1.777	0.26	M
13	17_6554	1.708	0.162	1.739	1.729	0.2	M
14	17_6555	1.707	0.162	1.719	1.73	0.17	M
15	17_6556	1.708	0.166	1.777	1.777	0.37	M
16	17_6557	1.708	0.164	1.741	1.748	0.25	M
17	17_6558	1.707	0.163	1.722	1.741	0.2	M
18	17_6559	1.71	0.159	1.693	1.692	0.17	M
19	17_6560	1.708	0.166	1.785	1.78	0.36	M
20	17_6561	1.707	0.167	1.783	1.786	0.25	M
21	17_6562	1.707	0.163	1.743	1.736	0.19	M
22	17_6563	1.707	0.161	1.732	1.72	0.16	M

Figure 2.18: CH₄ concentration ($\mu\text{mol/mol}$); PUP, Parcel 1, 30/03/2022

Name:		Coleta 17			Created On:	06/Apr/22 15:06:41	
Directory:		BOTICARIO			Created By:	Embrapa Floresta GC	
Data Vault:		Embrapa_set_18			Updated On:	19/Apr/22 08:08:38	
No. of Injections:		156			Updated By:	Embrapa Floresta GC	
By Component		N2O					
No.	Injection Name	Ret.Time min	Area kHz*min	Height kHz	Amount	Rel.Area %	Peak Type
		BackDetector	BackDetector	BackDetector	BackDetector	BackDetector	BackDetector
		N2O	N2O	N2O	N2O	N2O	N2O
1	P1	3.858	0.047	0.29	265.801	100	M
2	P1	3.87	0.045	0.276	243.175	100	M
3	P2	3.863	0.082	0.493	552.487	100	M
4	P2	3.865	0.083	0.499	557.983	100	M
5	P3	3.863	0.142	0.839	1050.71	100	M
6	P3	3.87	0.136	0.804	996.844	98.19	M
7	17_6548	3.887	0.056	0.331	333.569	100	M
8	17_6549	3.867	0.057	0.348	344.111	100	M
9	17_6550	3.87	0.058	0.349	353.039	100	M
10	17_6551	3.873	0.058	0.356	350.573	100	M
11	17_6552	3.868	0.055	0.335	328.83	100	M
12	17_6553	3.863	0.057	0.343	341.593	100	M
13	17_6554	3.87	0.055	0.343	330.52	100	M
14	17_6555	3.875	0.057	0.345	348.699	100	M
15	17_6556	3.868	0.055	0.334	324.293	100	M
16	17_6557	3.872	0.055	0.339	328.913	94.68	M
17	17_6558	3.865	0.055	0.337	330.788	95.13	M
18	17_6559	3.868	0.055	0.339	324.814	100	M
19	17_6560	3.865	0.056	0.337	333.513	100	M
20	17_6561	3.87	0.06	0.368	371.726	100	M
21	17_6562	3.88	0.066	0.4	419.561	100	M
22	17_6563	3.868	0.071	0.426	460.342	100	M

Figure 2.19: N₂O concentration ($\eta\text{mol/mol}$); PUP, Parcel 1, 30/03/2022

Name:		Coleta 17			Created On:	06/Apr/22 15:06:41	
Directory:		BOTICARIO			Created By:	Embrapa Floresta GC	
Data Vault:		Embrapa_set_18			Updated On:	19/Apr/22 08:16:06	
No. of Injections:		156			Updated By:	Embrapa Floresta GC	
By Component		CO2					
No.	Injection Name	Ret.Time min	Area pA*min	Height pA	Amount	Rel.Area %	Peak Type
		FrontDetector	FrontDetector	FrontDetector	FrontDetector	FrontDetector	FrontDetector
		CO2	CO2	CO2	CO2	CO2	CO2
1	P1	3.65	26.67	111.111	322.897	99.78	M
2	P1	3.648	26.001	108.01	313	99.79	M
3	P2	3.65	37.338	155.315	480.865	99.75	M
4	P2	3.65	37.885	158.088	488.959	99.75	M
5	P3	3.648	96.633	401.449	1358.823	99.71	M
6	P3	3.648	93.637	388.653	1314.456	99.71	M
7	17_6548	3.622	46.598	194.123	617.967	99.63	M
8	17_6549	3.653	72.513	301.92	1001.685	99.78	M
9	17_6550	3.653	92.276	383.778	1294.31	99.83	M
10	17_6551	3.653	106.782	443.139	1509.089	99.85	M
11	17_6552	3.655	43.385	180.563	570.398	99.61	M
12	17_6553	3.653	62.918	261.965	859.615	99.74	M
13	17_6554	3.653	80.608	335.793	1121.539	99.8	M
14	17_6555	3.652	95.677	398.412	1344.661	99.83	M
15	17_6556	3.653	44.853	186.727	592.137	99.63	M
16	17_6557	3.653	64.714	269.284	886.203	99.75	M
17	17_6558	3.652	81.05	337.375	1128.086	99.8	M
18	17_6559	3.653	91.94	381.906	1289.33	99.83	M
19	17_6560	3.652	46.294	192.615	613.464	99.64	M
20	17_6561	3.652	66.911	278.298	918.732	99.75	M
21	17_6562	3.65	85.129	353.377	1188.486	99.81	M
22	17_6563	3.652	102.868	426.997	1451.134	99.84	M

Figure 2.20: CO_2 concentration ($\mu mol/mol$); PUP, Parcel 1, 30/03/2022

2.4 Calculus

The concentrations are transformed in $\mu L_{CH_4}/L_{gas}/min$ or $\eta L_{N_2O}/L_{gas}/min$ or $\mu L_{CO_2}/L_{gas}/min$, which represent the gases rates of change in time inside the chamber (dN/dt). This is operated by means of the excel function @LINEST which, by means of the different measurement times (e.g 0, 20, 40, 60) and the relative concentrations, provides a single value considering a linear fit model.

Similarly, is computed the R^2 statistical value through the function RSQ; it returns the square of the Pearson product-moment correlation coefficient through data points (4 concentrations and 4 collection times). By using this coefficient, it is possible to identify outliers; some thresholds are set: 0.8 for CH_4 , 0.7 for N_2O and 0.8 for CO_2 . If the R^2 is lower than the threshold, it's necessary to remove the point (one of the 4 concentrations) that, when deleted, leads to the configuration with the higher R^2 . When the value is removed, the interpolation performed with @Linest is updated on the remaining data (3 concentrations). Eventually, the whole chamber data of the considered gas are discharged if, after removing the value, the R^2 is still lower than: 0.7 for CH_4 , 0.5 for N_2O and 0.7 for CO_2 .

A low deletion rate (less than 2%) has been observed in this study case.

In most cases, data anomalies are caused by failures in handling the syringe or leaks in the vial septum.

Flux calculus

For simplicity, only N_2O will be named from now on; however, all considerations also apply to CH_4 .

A flux calculation (FC) method must be selected.

The presence of the chamber on the soil affects gas diffusion. This effect leads to non-linearity in the relationship between concentration and time, such that the maximum value of the slope dN/dt occurs immediately after chamber placement and decreases over time. A Linear regression FC method is anyhow adopted because, compared with other FC schemes, LR-based estimates are least sensitive to random variations arising from ‘measurement error’ (Venterea et al. 2009) and have the lowest method detection limit (T. B. Parkin et al. 2012). In this sense, LR can be said to have greater precision, while at the same time having the greatest bias. Precision measures how similar the estimates are to each other; bias measures how close they are to the true value. However, under certain circumstances, precision can be considered of greater importance than bias. In this regard, Venterea et al. 2009, showed that LR-based flux estimates can be more statistically robust for detecting differences in fluxes among experimental treatments, by reducing the additional variance contributed by measurement error.

The linear regression flux calculation method is also selected because of its simplicity of application. The LR principle is to use the slope obtained from least-squares linear regression of N versus t to estimate dN/dt ; thus, the flux can be calculated directly as:

$$F = \frac{V}{A} \cdot \frac{dN}{dT} \quad (2.3)$$

Accordingly, the flow (emission or consumption) is computed through the formula:

$$flow(\mu gN/m^2/h) = \left(\frac{\frac{dN}{dt} \cdot V}{A} \cdot \frac{P_{atm}}{R \cdot T} \cdot 60 \cdot M \right) / 1000 \quad (2.4)$$

where: dN/dt = gas rate of change in the chamber ($\eta L_{N_2O} / L_{gas} / min$); V = chamber volume (L) = 33; A = chamber area (m^2) = 0.083; T = average temperature inside each chamber (K); P_{atm} = atmospheric pressure (atm) = 0.921; R = gas constant ($atm \cdot L \cdot mol^{-1} \cdot K^{-1}$) = 0.0821; M = N_2 molar mass (g/mol) = 28.

Cumulative emissions

The estimation of cumulative emissions using non-continuous data needs to fill temporal gaps between measurement campaigns and to account for spatial variability.

Regarding **spatial variability**, large coefficients of variation are often encountered in flux data derived from static chamber: e.g. 50-100% for CH_4 and 13-57% for N_2O (Yamulki et al. 1995). This variability can be represented by log-normal distribution, normal distribution, more than one distribution for different periods of the year, distribution in clusters or by Kriging technique. However, the possibility of attributing the relevant distribution is limited when only a few chambers are used in a particular treatment. In this circumstance, as in this case study, a normal distribution is assumed and the emissions are estimated by arithmetic means (Cardenas et al. 2010).

The spatial standard deviations, which measure how widely the values are dispersed from the average, are computed for each measurement campaign and reported in figures 2.21 - 2.22 - 2.23.

NATIVE FOREST					
Coleta n°	Date	Average N2O (ug N/m2/h)	Stdev N2O (ug N/m2/h)	Average CH4 (ug C/m2/h)	Stdev CH4 (ug C/m2/h)
1	12/11/2019	49.384	67.722		
2	13/11/2019	25.692	39.009		
3	14/11/2019	55.748	87.740		
4	10/03/2020	15.128	16.182	7.807	93.418
5	11/03/2020	32.851	60.840	2.206	134.034
6	12/03/2020	16.555	12.904	42.443	52.879
7	22/06/2021	21.206	11.651	-10.499	11.878
8	23/06/2021	23.385	36.336	-17.018	17.555
9	24/06/2021	28.403	26.768	-17.541	14.121
10	18/08/2021	4.783	10.968	-23.970	16.511
11	19/08/2021	10.808	22.470	-11.940	42.536
12	20/08/2021	2.053	11.802	-22.709	13.991
13	19/10/2021	11.044	9.945	-16.854	25.449
14	20/10/2021	15.962	11.462	-24.104	16.460
15	21/10/2021	20.953	18.482	-22.151	16.980
16	29/03/2022	21.199	11.962	-57.236	34.186
17	30/03/2022	15.396	11.302	-40.731	28.000
18	31/03/2022	17.662	23.861	-36.044	29.914
19	17/05/2022	14.321	23.964	-46.735	41.151
20	18/05/2022	11.694	13.742	-28.460	20.366
21	19/05/2022	5.734	15.547	-42.474	24.328

Figure 2.21: Fluxes averages and σ ; NAT

PUPUNHA CULTURE					
Coleta n°	Date	Average N2O (ug N/m2/h)	Stdev N2O (ug N/m2/h)	Average CH4 (ug C/m2/h)	Stdev CH4 (ug C/m2/h)
1	12/11/2019	805.229	472.437		
2	13/11/2019	9.590	6.453		
3	14/11/2019	10.084	24.695		
4	10/03/2020	100.537	73.533	-25.188	9.764
5	11/03/2020	126.757	57.227	8.252	35.856
6	12/03/2020	99.662	55.515	-17.733	10.559
7	22/06/2021	6.430	18.765	-7.921	8.264
8	23/06/2021	1.955	17.283	-2.032	7.185
9	24/06/2021	12.470	17.416	5.851	31.982
10	18/08/2021	42.812	94.547	-3.808	7.364
11	19/08/2021	8.339	10.071	-8.320	9.595
12	20/08/2021	7.439	10.528	-8.786	12.442
13	19/10/2021	3.764	7.852	2.182	6.453
14	20/10/2021	6.098	8.448	0.364	9.511
15	21/10/2021	4.946	6.932	-3.732	13.528
16	29/03/2022	43.794	36.711	-10.431	7.263
17	30/03/2022	44.738	34.271	-11.032	6.880
18	31/03/2022	33.215	36.038	-11.962	19.972
19	17/05/2022	21.046	23.241	-16.072	8.323
20	18/05/2022	12.324	17.493	-13.735	6.171
21	19/05/2022	23.313	29.580	-15.871	6.615

Figure 2.22: Fluxes averages and σ ; PUP

REGENERATED FOREST					
Coleta n°	Date	Average N2O (ug N/m2/h)	Stdev N2O (ug N/m2/h)	Average CH4 (ug C/m2/h)	Stdev CH4 (ug C/m2/h)
1	12/11/2019	21.836	28.463		
2	13/11/2019	281.733	446.444		
3	14/11/2019	164.999	87.198		
4	10/03/2020	0.954	22.796	-43.043	22.036
5	11/03/2020	10.132	11.399	47.885	43.705
6	12/03/2020	8.693	20.954	-46.625	15.446
7	22/06/2021	4.333	14.189	-24.008	12.075
8	23/06/2021	-3.437	33.172	-19.896	17.014
9	24/06/2021	1.641	15.026	-22.530	12.452
10	18/08/2021	6.450	15.261	-23.123	10.796
11	19/08/2021	0.192	19.244	-22.801	11.480
12	20/08/2021	1.318	7.639	-19.371	26.083
13	19/10/2021	1.640	8.913	-14.801	12.974
14	20/10/2021	4.329	6.102	-20.327	9.958
15	21/10/2021	5.489	9.804	-21.149	9.834
16	29/03/2022	3.813	5.936	-33.560	16.582
17	30/03/2022	4.651	12.085	-33.451	14.505
18	31/03/2022	14.488	12.338	-7.956	38.186
19	17/05/2022	6.712	11.728	-28.672	14.353
20	18/05/2022	5.203	7.719	-28.333	14.808
21	19/05/2022	4.086	4.292	-26.698	10.870

Figure 2.23: Fluxes averages and σ ; REG

Concerning instead the **filling of temporal gaps** between measurement campaigns to obtain cumulative flows over the representative year, two different merging methods are investigated in the following paragraphs.

Method 1

In order to cumulate the data, the daily fluxes are here merged over the monitoring period using trapezoidal integration, corresponding to the area under the curve. To gain greater accuracy, the curve is computed on close collection dates only. For this reason, the measuring campaigns of November 2019 and March 2020 are discarded and the period considered is June 2021 - May 2022, an appropriate time window to consider all seasons of the year.

The areas of the trapezoids are the product of the time distance between two collections (x-axis) and the medium gas flux of these two (y-axis); figure 2.24.

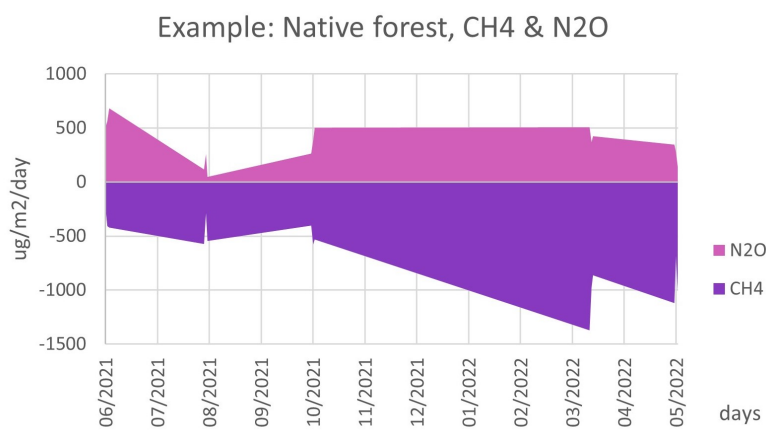


Figure 2.24: Method 1 calculation principle

The areas are subsequently summed, divided by the collection period June 2021 - May 2022 (331 days) and multiplied by 365 days/year; this leads to the estimate of the annual “mean” CH_4 and N_2O fluxes, whose values are reported later in figures 2.26 - 2.27 in the paragraph concerning the methods comparison.

Method 2

This technique makes use of weighted averages over the seasons.

The measurement campaigns considered are:

- March 2020 and March 2022 → summer,
- June 2021 and May 2022 → autumn,
- August 2021 → winter,
- October 2021 → spring.

It is assumed that the averages of the various collections made in each season are representative values of each; figure 2.25.

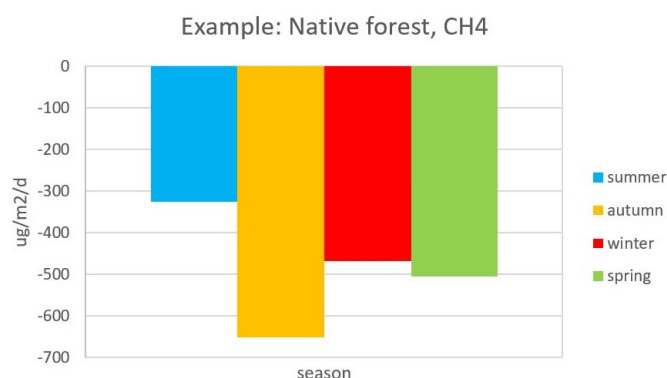


Figure 2.25: Method 2 calculation principle

Finally the cumulation is carried out by multiplying each of the averages for the duration of a season (91 days), allowing to obtain the estimate of the annual “mean” CH_4 and N_2O fluxes whose values are reported later in figures 2.26 - 2.27 in the paragraph concerning the methods comparison.

Methods comparison

Measurement campaigns have been organized by collection dates. However, since the aim of this study is to assess the net carbon balance of a territory, the data are reorganized by parcels and cameras. This way it becomes possible to gather, along with the flux results, the standard deviations which describe the spatial dispersion of the outcomes; the final values are reported in table 2.1 .

This way, figures 2.26-2.27 are generated, allowing to present the results of both methods and to proceed with the dissertation whose goal is to pick the most accurate calculation procedure.

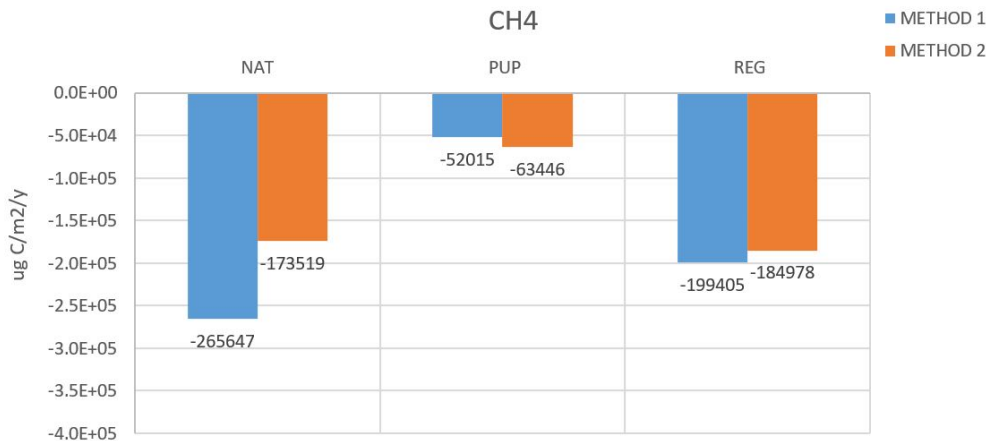


Figure 2.26: CH_4 results of both methods



Figure 2.27: N_2O results of both methods

Some considerations arise. The procedure of trapezoidal integration (method 1) appears to be more rigorous than season-based subdivision (method 2), since it encompasses 14 areas rather than 4 as in method 2. This would lead to conclude that method 1 is the one to prefer. However, it presents one problematically long interval between two collections (more than 5 months), which may result in significant overestimation; with method 2, on the other hand, constant intervals of 3 months have been established.

As a consequence of the conflicting statements discussed above, it's considered as best estimate the average of the results coming from both methods.

2.5 Results

The final outcomes, that is the average of the results of the two explored methods, are finally reported in figure 2.28.

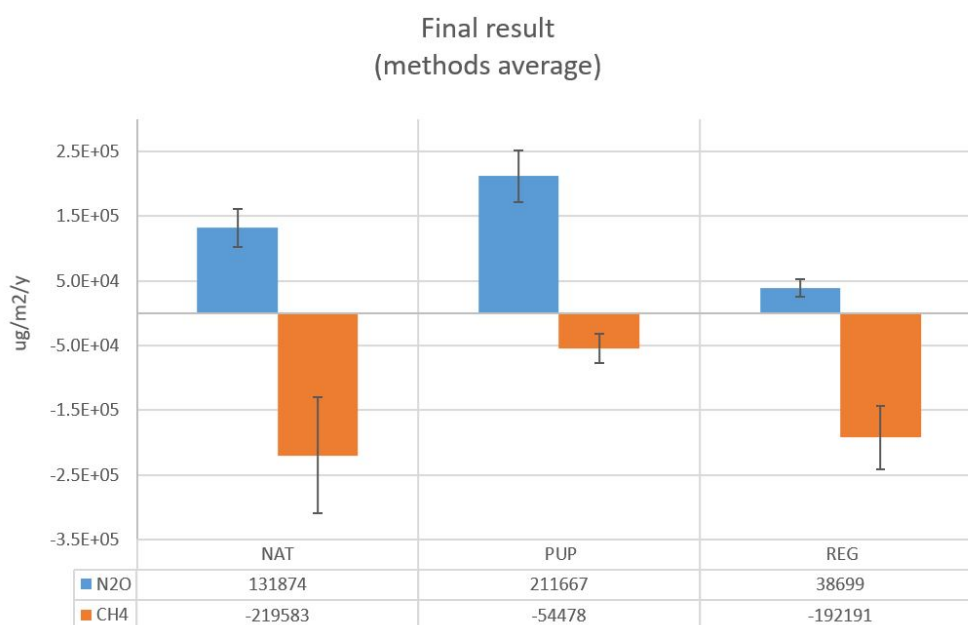


Figure 2.28: Methods average results

It's interesting to report the values' dependence on the measurement season; to do so, method 2 technique is utilized, resulting in the flux distribution of figure 2.29.

The mitigation potential of GHGs emissions is assessed by means of the global warming potential GWP, which is an equivalent of CH_4 and N_2O in relation to CO_2 of 28 and 265 times respectively (Hiraishi et al. 2014). Figure 2.30 and table 2.1 report the final GHGs fluxes with the associated spatial standard deviations, in CO_2 -equivalents.

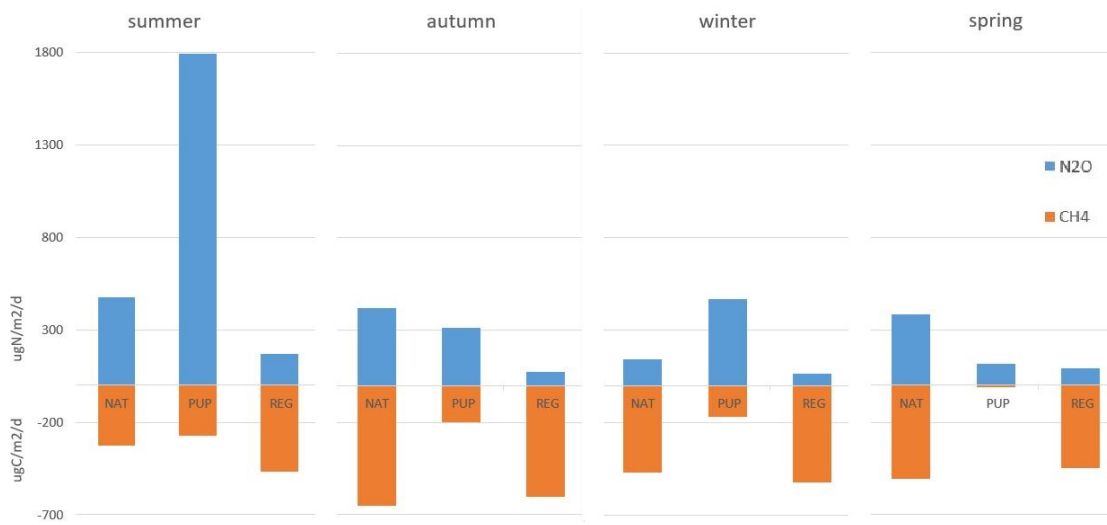


Figure 2.29: Season-dependent flux trend

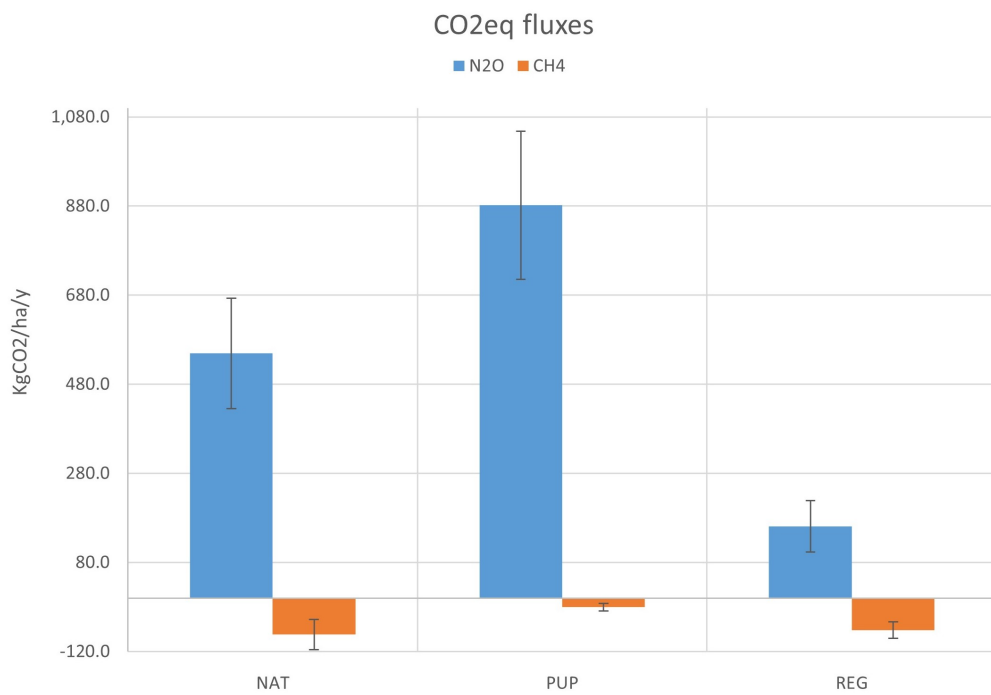


Figure 2.30: GHGs fluxes and σ in CO_2 equivalent

NAT	N_2O ($KgCO_2/ha/y$)	CH_4 ($KgCO_2/ha/y$)
	549±248	-82±67
PUP	N_2O ($KgCO_2/ha/y$)	CH_4 ($KgCO_2/ha/y$)
	881±332	-20±16
REG	N_2O ($KgCO_2/ha/y$)	CH_4 ($KgCO_2/ha/y$)
	161±116	-72±37

Table 2.1: GHGs fluxes and σ in CO_2 equivalent

2.6 Result discussion

Moving towards reaching the goal of this study, the following comments emerge:

- Nitrous oxide flux constitutes an emission.
- N_2O emission is the lowest in REG, for all seasons. This possibly reflects the condition of the soil in regenerated forest plots which present lower supply of oxygen due to the high water table, causing N_2 losses in the form of gas.
- N_2O flux is substantially high in summer in PUP.
- Methane flux represents an influx, that is the absorption of CH_4 by the soil.
- CH_4 influx is very similar between NAT and REG, meaning the methane stored in Regenerated forest stand is almost replenished compared to the unaltered forest; the same cannot be said for PUP.
- The largest CH_4 influx is observed in autumn in NAT.

Literature check

Reference values of N_2O and CH_4 fluxes are consulted for Atlantic native forest (Silva et al. 2022) and reported:

$$N_2O = 0.1 \text{ mg}/m^2/d = 23227 \text{ ugN}/m^2/y \rightarrow !$$

$$CH_4 = -0.84 \text{ mg}/m^2/d = -229950 \text{ ugC}/m^2/y \rightarrow \text{ok}$$

The intake of methane is validated, while the nitrous oxide flux turns out to be much higher than in literature; however, this is explained by the great variability of forest characteristics.

Regarding REG and PUP stands, literature data are missing, underlining the importance of the outcomes achieved in this study.

Chapter 3

Soil organic carbon

3.1 Introduction

Organic carbon is the major constituent of soil organic matter (SOM), which plays pivotal roles in soil attributes like cation exchange capacity, nutrient cycling, stabilization of aggregates, water retention capacity and biological activity.

The soil organic carbon (SOC) pool also functions as a sink for atmospheric carbon and contributes to mitigating anthropogenic GHGs emissions, provided that soil is properly managed. SOC stock depend on several factors like soil type, climate, tree species, previous land-use system, site preparation method and forest management practices. Depending on how those factors are combined, effects on SOC of cultivation and regeneration vary broadly in depletion or restoration, relative to the baseline native forest.

It is essential to use a common, simple and low-cost method to assess soil carbon stock; in view of this compliance, a Protocol (Zanatta et al. 2015) is abided. There, the sampling strategies are consistent with the principles of the Intergovernmental Panel on Climate Change (IPCC), which requires quality in terms of collection, documentation, archiving and retrieval, in addition to standardized procedures.

In order to estimate the SOC the soil density it's also computed; furthermore, the nitrogen content is evaluated being a parameter that enriches the discussion on carbon accumulation and soil carbon dynamics.

3.2 Sampling

Instrumentation

Soil bulk density is determined by the dry mass of a sample of known volume, thus making use of the volumetric core method; the methodology follows the procedures described in Embrapa manual (Donagema et al. 2011).

The sample, with undisturbed structure, is collected by the 'Steel ring of Kopecky' tool, with 50 mm high rings for all layers; figures 3.1 and 3.2.



Figure 3.1: Kopecky tool



Figure 3.2: Kopecky 50 mm steel rings

C&N content determination makes use of the 'Dutch auger' tool, figure 3.3.

Notes

- To carry out both measurements easily and with results as consistent as possible with reality, the campaign is executed under equitable soil moisture conditions.
- While sampling surface layers in forest soils, attention must be paid to the presence of litter and necromass; fragments and roots, even in low amounts, may in fact result in overestimated carbon levels.
- While collecting, care is taken to not contaminate the samples from lower layers with soil from surface layers, which generally has higher carbon content.



Figure 3.3: Dutch auger tool

Sampling intensity

The measurement design includes 3 parcels for each forest stand (NAT/REG/PUP), 10 or 8 layers investigated respectively for density and C&N determination until 1 m depth (figure 3.4), and 2 rings (A and B) collected per layer; for a total of 144 samples.

Regarding temporal intensity, as soil parameters are little variable in time, only one campaign has been carried out, performed in October 2019 for density and in December 2021 for C&N content.

Parcels location

The plot is intended, in this case, as the single perforation from which the samples at different heights are extracted.

Density and C&N measuring ports are drilled next to each other, furthermore, their location is close to GHGs measuring points (figures 2.4-2.5-2.6 in Chapter 2), thus the GPS maps are not reported.

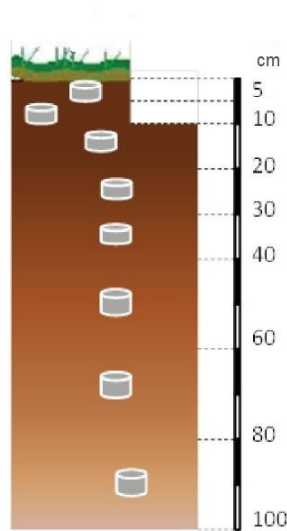


Figure 3.4: Sampled layers for C&N determination

Sampling steps

Soil bulk density

The Kopecky tool is inserted by percussion into the soil until the designated depths, then the soil samples are pulled outside and inserted in labelled plastic bags for laboratory handling. Great care is taken by the operator to avoid the compaction of the sample inside the ring and in the cleaning action consisting in removing excess soil from the ring edges.

C&N content

The Dutch auger tool is inserted into the soil by rotation until the designated depths, then the soil samples are pulled outside and inserted in labelled plastic bags for laboratory analysis. 300 - 500 g_{dry} of soil are collected, being this mass sufficient for the analyses and still allowing material storage for future studies.

3.3 Laboratory analysis

Soil bulk density

The laboratory handling for density investigation only consists in preparing the samples for the calculation reported in section 3.4. The operations just include

sample weighing (by vacuum scale with 5 decimal places of gram precision) and drying (in an oven at 105°C for 48 h).

C&N content



Figure 3.5: Elementar ®Vario MACRO Cube analyzer

The calculation of SOC, and also litter carbon (discussed later in Section 4.5), is performed through laboratory analysis. The instrumentation employed by Embrapa consists of an Elementar ®Vario MACRO Cube analyzer (figure 3.5).

Vario MACRO Cube is a simultaneous one-sample N, C, H and S analyzer. The application covers all organic and the majority of inorganic samples of solid or liquid form. The instrument's strengths are its weight flexibility (micro and macro range), low detection limit, dynamic concentration range and ability to handle heterogeneous samples. All instrument functions are digitally controlled and monitored; permitting automatic operation, optimization, and remote management and diagnosis. Furthermore, the software includes automatic leak test, extensive error diagnosis, monitoring of maintenance cycles, a sleep/wake-up function, statistical evaluation, and almost unlimited memory capacity.

The laboratory analysis steps for the determination of C&N content are:

Step 1: the soil collected is dried in metal vessels in the oven at 40 °C for 72 h.

Step 2: the sample is ground to 2 mm.

Step 3: a portion of 100 grams is ground to 0.25 mm in order to fit the CHNS elemental analyzer.

Step 4: the analysis with the Elemental analyzer (CHNS) now starts. For each sample about 40 mg of soil, now grounded and dried, are placed in small containers made of tin (inert), these latter closed by pinching the end and loaded in the machine carousel.

Step 5: the content automatically falls into a ball valve for blank-free transfer (figure 3.6 b-c).

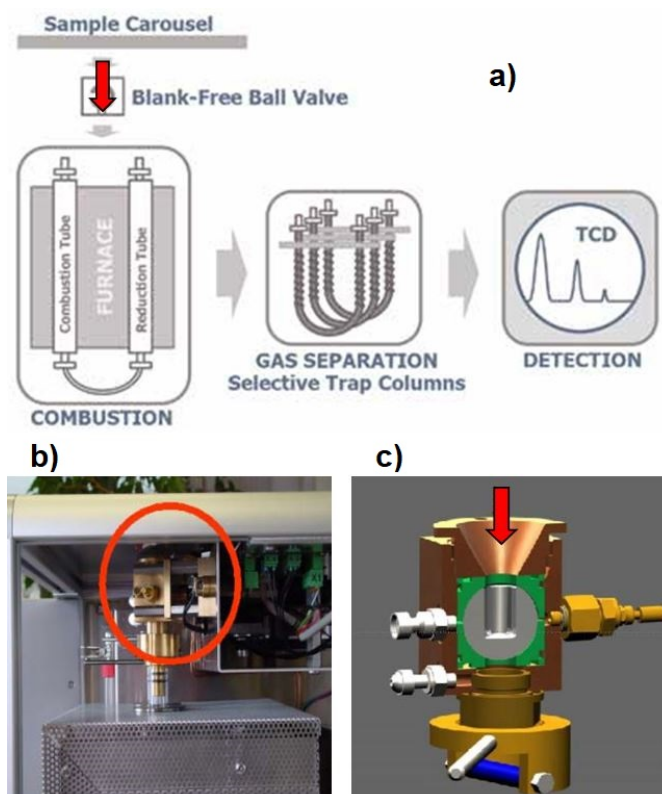


Figure 3.6: a) CHNS Analyzer scheme; b) ball valve; c) ball valve scheme

Step 6: the valve turns 90° and a flow of helium carrier gas runs in order to remove atmospheric nitrogen, resulting in a zero blank sampling process.

Step 7: the valve turns further and releases the sample which falls into the catalytic combustion tube inside which there is a ceramic tubular crucible (figure 3.7b). Inside the combustion column is present an O_2 injection lance (figure 3.7c); the direct flux (emitted continuously at 1150 °C) to the sample leads to the highest oxygen concentrations at the point of combustion (ensuring total combustion), as

well as low gas consumption.

The result is a blend of ash, containing alkaline earth metals in mineral form, and gas, which is the analysis target.

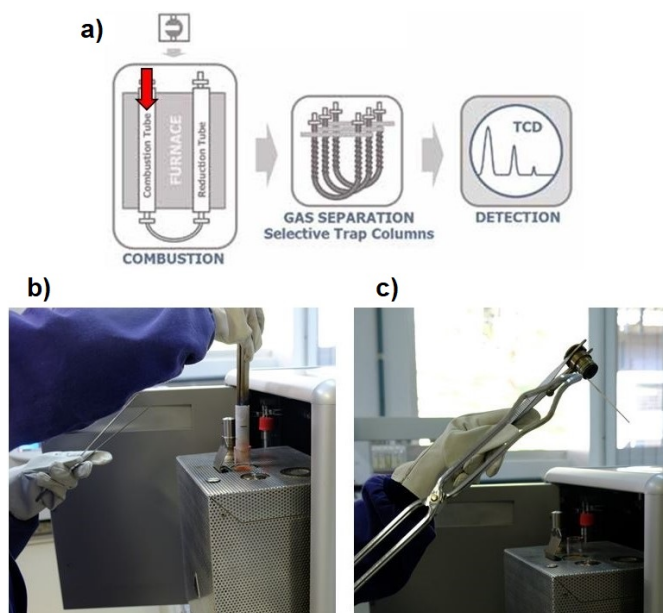


Figure 3.7: a) CHNS Analyzer scheme; b) ceramic tubular crucible; c) O_2 injection lance

Step 8: it follows the reduction of the combustion gases in the reduction tube, this takes place on hot copper, which gives the column its characteristic color (figure 3.8b). The formed analyte gases, N_2 , CO_2 , H_2O and SO_2 , remain in the He carrier gas stream.

Step 9: the gases reach two drying cylinders containing agents whose purpose is the removal of water (figure 3.9). The content of the cylinders changes from white to blue during usage.

Step 10: the gas mixture now travels through three Advanced purges & trap (APT) columns for gaseous components separation, trapping SO_2 , H_2O and CO_2 in order of crossing (figure 3.10b).

The APT technology is the leading chromatographic technique for the determination of non-metal elements; in conjunction with the detection of the combustion flux without gas splitting and dilution, the technology is capable of resolving C/N ratios of up to 7000:1.

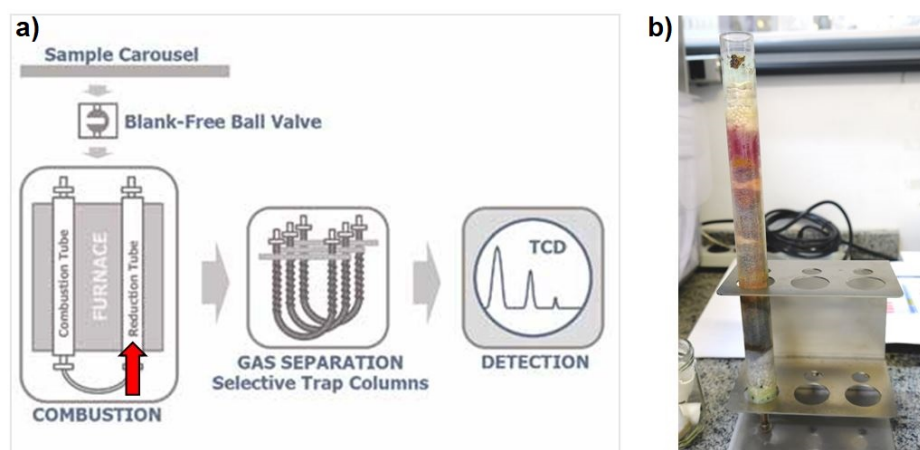


Figure 3.8: a) CHNS Analyzer scheme; b) copper reduction tube



Figure 3.9: Analyzer drying cylinders

The adsorption of combustion gases on the three separation columns and the subsequently controlled desorption grant a wide dynamic range that allows for the sequential analysis of very high concentrations next to very low ones, ensuring 100% detection for concentration < 100 ppm.

CO_2 , H_2O and SO_2 are sequentially adsorbed on specific columns. N_2 passes through all three columns and goes toward the detector TCD (see Step 11). After the detection of the N_2 peak, the CO_2 column is quickly heated; CO_2 is released to the TCD. H_2O column is then heated and the desorbed gas is diverted directly to the TCD. Finally, the SO_2 column is heated and the gas, by-passing the other two columns, is quantified by the TCD.

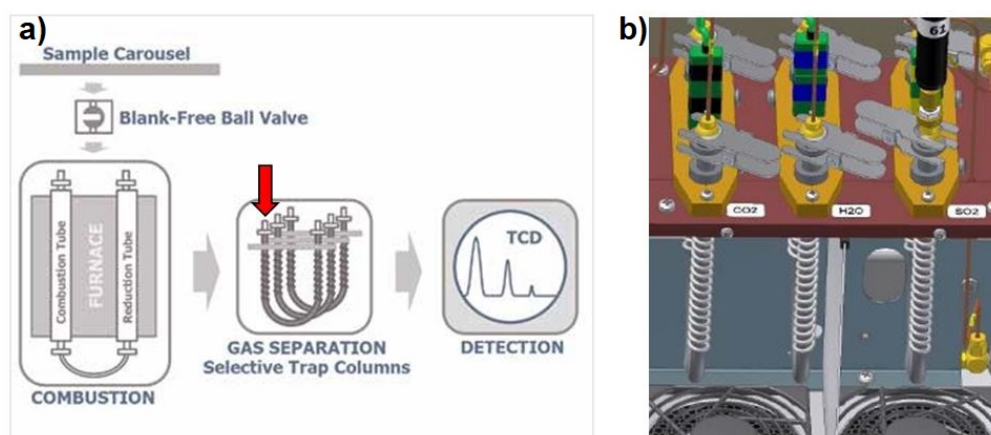


Figure 3.10: a) CHNS Analyzer scheme; b) APT columns

Step 11: the gases (in the order reported above and in figure 3.11b), reach the thermal conductivity detector TCD, which utilizes thermistors. An electronic gas flow controller is positioned just before the detector ensuring stable pressure and flow conditions, resulting in a multi-point calibration with linear regression to the 4th order which keeps the instrument stable over months.

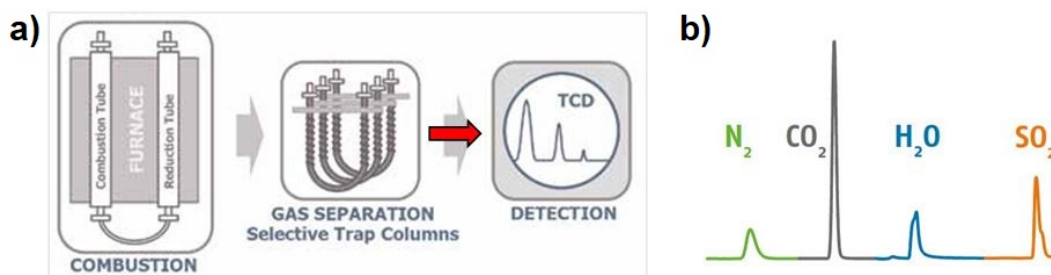
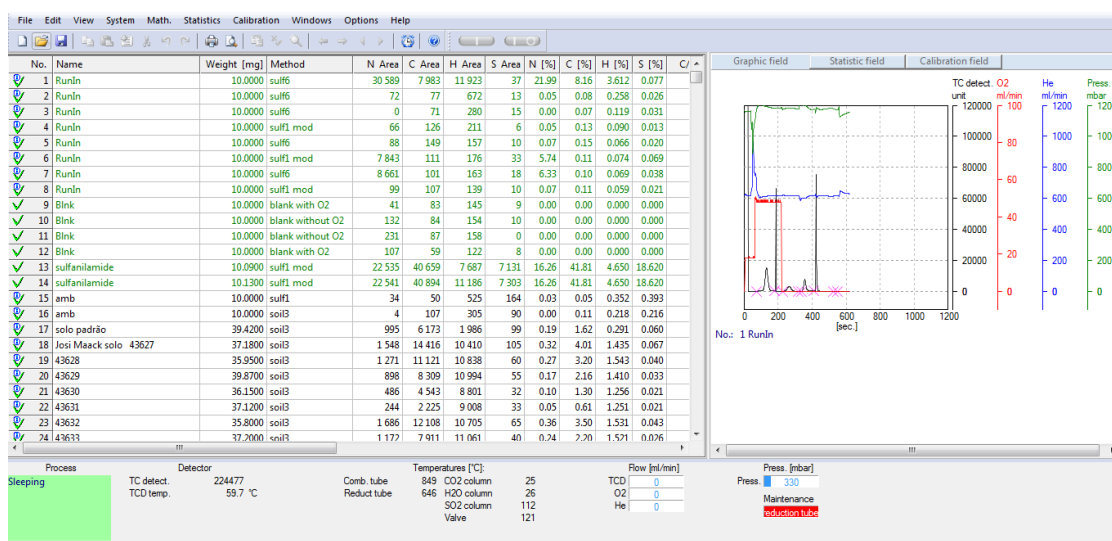


Figure 3.11: a) CHNS Analyzer scheme; b) detected gases

The desired outputs can now be derived. The gas sign is recognized thanks to the different thermal conductivity, appearing on graph as an area ($sec \cdot ml/min$). The Elemental analyzer firmware computes the percentage weights of elements based on calibration curves of standards with known concentrations of CHNS; a screenshot is displayed in figure 3.12.

As a result of laboratory analysis, CHNS results were obtained; for the purpose of this study however, only C and N contents are relevant and therefore afterwards reported.



186. Name: amb N [%]: 0.04 C [%]: 0.06 H [%]: 0.433 S [%]: 0.057

Figure 3.12: Elemental analyzer firmware output

3.4 Calculus

Soil density analysis

For each sample the density it's derived as:

$$D_s = \frac{a}{b} \tag{3.1}$$

Where: D_s = soil density (g/cm^3); a = dry sample mass;

b = ring volume = $(\pi \cdot r^2) \cdot h = (\pi \cdot 2.52) \cdot 5.3 = 104.07 \text{ cm}^3$

C&N analysis

- From the C&N percentages obtained through the Elementar analyzer, the averages for each parcel for each layer for each forest stand are derived.
- The C&N stocks are calculated by the product of the thickness of the layer, the C or N percentage and the density.
- The depth cumulate of the stocks it's also computed summing the stocks as proceeding with depth.
- As a reference the native forest data are used. The mass of the reference stand is computed by the product of the reference density and the layer thickness. Furthermore the reference depth cumulate of mass it's calculated.
- The mass is computed by the product of the layer thickness and the corresponding density. The cumulate of mass with the depth it's computed too.
- Finally the accumulated C in each layer is calculated using the equivalent soil mass method (Ellert and Bettany 1995; Sisti et al. 2004). The same considerations are applicable to nitrogen.

The formula is:

$$\sum C_{\text{corr}}(Mg/ha) = \sum C_{i-1} + [m_i - (\sum m_i - \sum m_{ref_i}) \cdot \%C_i] \quad (3.2)$$

- The stock in each layer is the difference between $\sum C_{\text{corr } i}$ and $\sum C_{\text{corr } i-1}$.
- For each layer of each forest stand, the averages are calculated. In the results paragraph 3.5, the graphs (figures 3.13 - 3.14 - 3.15) show their dependence with depth.
- The C&N stocks for the layers 0-30 cm and 0-100 cm are calculated by the sum of the corresponding layers' data (figures 3.16 - 3.17). Note that C&N of the 0-30 cm soil layer is the reference for soil carbon inventories used by Eggleston 2006.
- Finally the C sequestration rate ($tC/ha/year$) is computed as difference with the reference C stock of native forest stand. REG carbon sequestration rate is computed by dividing the $\Delta carbon\ stock$ by 29 (years of forest succession), for PUP dividing by 24 (years since pasture introduction); figure 3.18.

3.5 Results

The outcomes from the analysis of all stands are here reported.

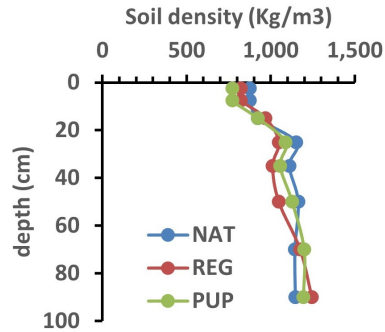


Figure 3.13: Soil density as a function of depth

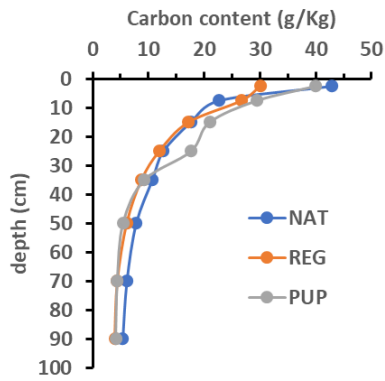


Figure 3.14: Carbon content as a function of depth

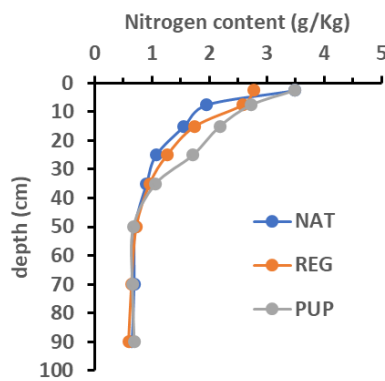


Figure 3.15: Nitrogen content as a function of depth

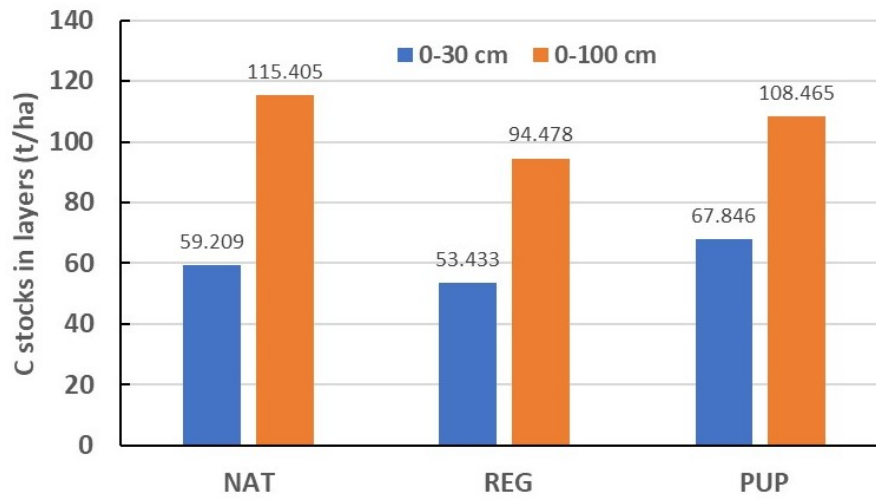


Figure 3.16: Carbon stock in different layers

The SOC results, that is to say the cumulates of C stocks in layers interval 0-30 cm, are reported in table 3.1.

Land-use	SOC (t/ha)
Native forest	59.21 ± 8
Regenerated forest	53.43 ± 3
Pupunha culture	67.85 ± 11

Table 3.1: Soil organic carbon and Standard deviation

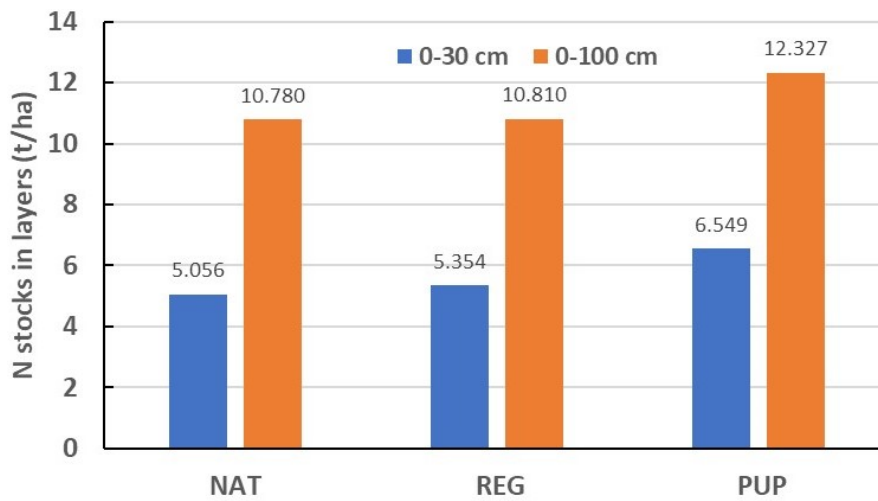


Figure 3.17: Nitrogen stock in different layers

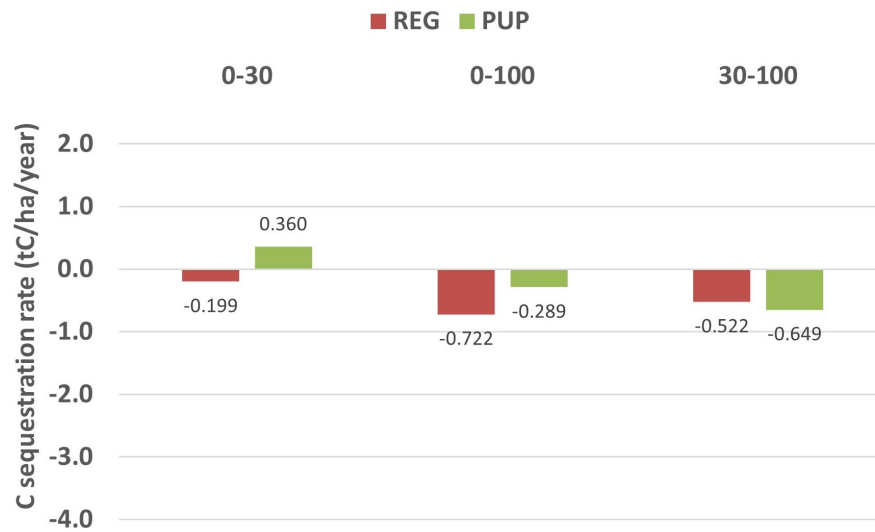


Figure 3.18: NAT-related carbon sequestration rate

The ΔSOC in relation to unaltered forest for the layers interval 0-30 cm, are reported in table 3.2, in CO_2eq .

Land-use	ΔSOC ($KgCO_2/ha/year$)
Regenerated forest	-730
Pupunha culture	1320

Table 3.2: NAT-related SOC in $CO_2equivalent$

3.6 Results discussion

The hypothesis expressed in the introduction of this study is that different stands would present decreasing values of carbon stock in relation to greater anthropization; in this regard is well known that SOC is depleted because of the following reasons:

- o intense soil disturbance \rightarrow disruption of the stable aggregates exposes the once occluded organic matter to a more oxidative environment and thus accelerates its decomposition.
- o low carbon input into the soil during the first years of regeneration \rightarrow litter input is minimal compared to NF.
- o lower decomposition rate of the forest floor in the regenerating area \rightarrow because of that, litter-C remains in the thick floor and the flux of carbon into the soil decreases.

The observation of the gained results leads to only partially confirm the hypothesis, in fact:

- In the 0-100 cm layer, NAT stores the largest stock of carbon, surprisingly followed by PUP and only after by REG (figure 3.16).

This is explained by the fact that before the Pupunha culture started in 2018, the area was used as pasture. This is known to bring increased carbon input due to animal droppings and to *Brachiaria* (for animal feed) root stimulation. Furthermore, during Peach palm cultivation the area potentially experienced fertilization.

Further comments are:

- Soil bulk density is almost uniform between the evaluated stands (figure 3.13).
- In all stands more than 50% of the carbon stock in the 0-100 cm layer is stored in the 0-30 cm interval (figure 3.16).

Literature check

Regarding the **density** output of the unaltered forest stand, a comparison with literature from Veloso et al., (M. G. Veloso et al. 2018) is conducted (figure 3.19); it validates the achieved trend.

Soil layer (cm)	NF
Bulk density (kg dm ⁻³)	
0-5 cm	0.65 ± 0.04
5-10	0.75 ± 0.07
10-20	0.93 ± 0.05
20-30	1.02 ± 0.02
30-45	1.12 ± 0.02
45-60	1.28 ± 0.01
60-80	1.28 ± 0.01
80-100	1.28 ± 0.01

Figure 3.19: unaltered forest density (M. G. Veloso et al. 2018)

Relating **C&N** results, the database contained in *Global Forest Resources Assessment (FRA) 2020* is exploited; there is stated 48,70 t/ha in the 0-30 cm depth interval, which validates the achieved value 59,2 t/ha.

Chapter 4

Forest carbon inventory

4.1 Introduction

The objective of this chapter is to assess the capacity of Dense Ombrophilous Atlantic forest to accumulate carbon in biomass. The intergovernmental panel on climate change has produced methodological guidelines that are here followed and adapted.

In order to quantify the carbon coming from forest biomass, the inputs are divided into four compartments: above ground, root, litter, and necromass.

4.2 Parcels settings

The plots are demarcated by means of a longitudinal main line of 25m and an offset of 5m on both sides. Because flat spots have been chosen (up to 2% slope), the distance on the terrain is assumed horizontal.



Figure 4.1: Parcel boundaries demarcation

The inventory design includes 7 parcels for NAT, 6 for REG and 1 for PUP, as displayed in figures 4.2 - 4.3 - 4.4 (the initial and final points of the transect are denominated respectively i and f).

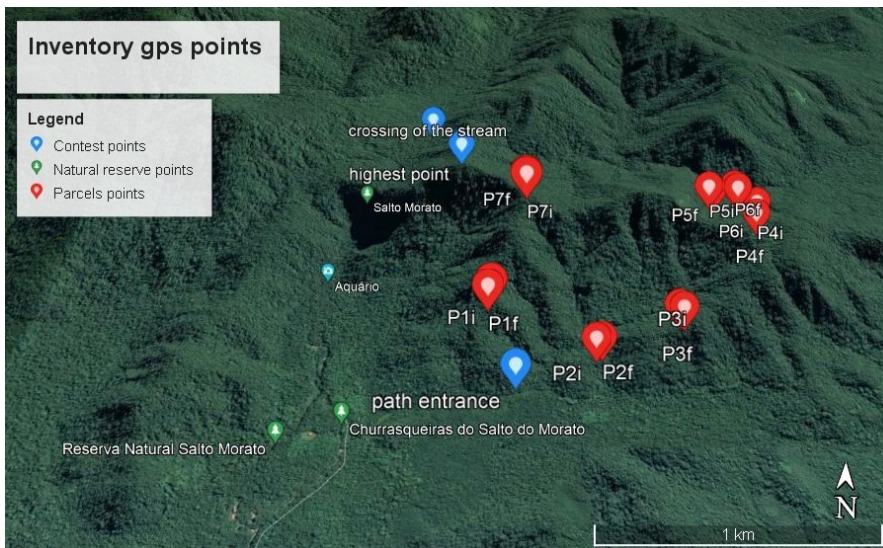


Figure 4.2: Inventory points in Native forest

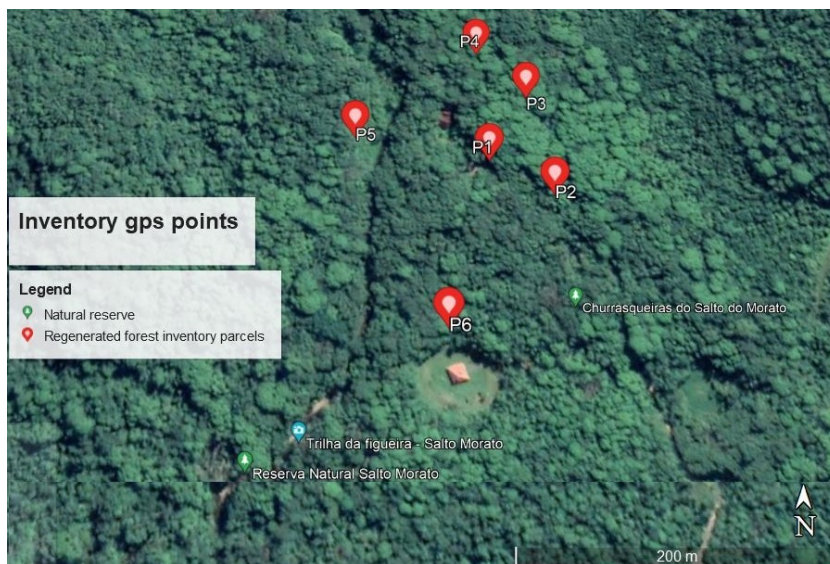


Figure 4.3: Inventory points in Regenerated forest

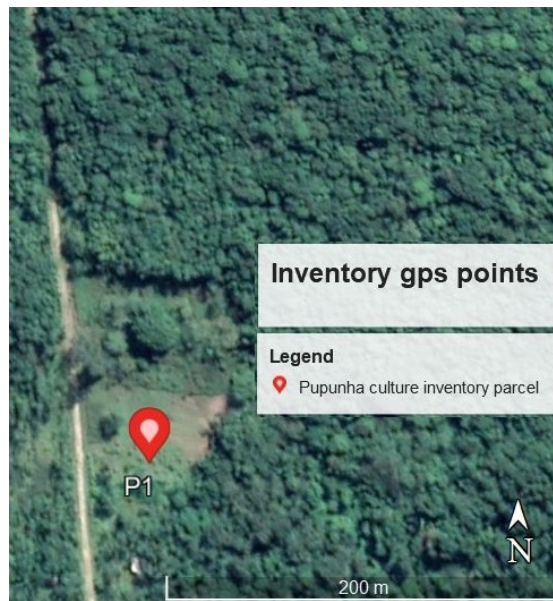


Figure 4.4: Inventory points in Pupunha culture

As for forest systems the “crop” dynamic is slow, only one campaign has been carried out for each forest stand; NAT biomass has been quantified in April 2022, while REG and PUP in July 2022.

The sampling intensity depends on the method envisaged for each compartment and will be reported in the dedicated paragraphs.

4.3 Aboveground compartment

Sampling

Within each parcel the following data are reported in the field forms:

- **Circumference at breast height (CBH)**
It's measured with a tape positioned parallel to the ground at 1.30 m. Some exceptions are shown in figure 4.5.
- **Height**
The plant's height is measured by means of a telescopic pole or by visual estimate by the expert botanist present in the team.
- **Species name**
The scientific name of the species is ascertained by the expert botanist.

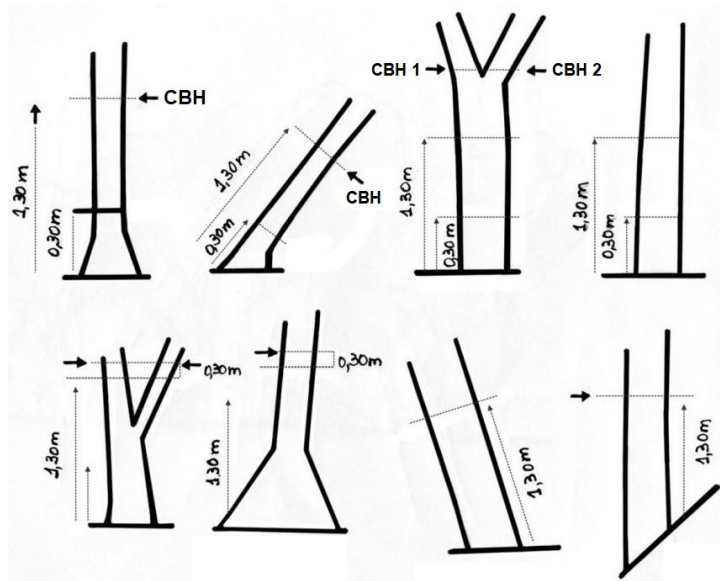


Figure 4.5: Circumference at breast height

If at the time of determining the species the botanist is not able to recognize the plant, a branch of it is taken with a pruning shear and prepared to be subsequently recognized in the laboratory (figure 4.6).



Figure 4.6: Branch for plant classification

Note that the collection of data for assessing aboveground biomass is performed after the one for litter and necromass, this in order to avoid the influence of team operators walking on the material to be quantified.

Biomass estimate

The best way to evaluate the dry aboveground biomass is by using allometric equations (indirect estimation method); this infers the biomass through extrapolation of easily obtainable variables at the plot level, such as diameter, height and wood density.

Relating **NAT and REG stands**, different formulas are chosen according to the geniuses (general trees, palms, arborescent ferns or cecropias) allowing us to take into consideration the different structure and density.

For general trees the allometric equation provided for the Atlantic forest by Tiepolo et al. 2002 is exploited, being calibrated in the State of Paraná, where this campaign is performed (figure 4.7).

Allometric models to estimate dry aboveground biomass (kg) for tropical forests. Biomass regression models may include trunk diameter DBH (in cm) and total tree height H (in m) and wood specific gravity “ρ” (in g.cm³).

Reference	Allometric model (AGB)	α	β ₁	β ₂	β ₃	R ²	DBH range (cm)
Allometric Model with 1 variable - DBH							
Chambers et al. (2001)	$= \exp(\alpha + \beta_1 \ln(\text{DBH}) + \beta_2 (\ln(\text{DBH}))^2 - \beta_3 (\ln(\text{DBH}))^3)$	-0.37	0.333	0.933	-0.1220	0.973	5-130
Burger (2005)	$= \exp(\alpha + \beta_1 \ln(\text{DBH}))$	-6.80067	3.77738	-	-	-0.915	12.5-27.9*
Tiepolo et al. (2002)	$= \alpha + \beta_1 (\text{DBH}) + \beta_2 (\text{DBH})^2$	21.297	-6.953	0.740	-	0.910	4-116
Allometric Model with 2 variables – DBH and wood density or DBH and Height							
Chave et al., (2005)a**	$= \rho \times \exp(\alpha + \beta_1 \ln(\text{DBH}) + \beta_2 \ln(\text{DBH})^2 - \beta_3 \ln(\text{DBH})^3)$	-1.499	2.1481	0.207	-0.0281	0.996	5-156
Scatena et al. (1993)	$= \exp(\alpha + \beta_1 (\ln(\text{DBH})^2 \times H))$	-3.282	0.95	-	-	0.947	2.5-57
Allometric Model with 3 variables - DBH, wood density, height							
Chave et al., (2005)b*	$= \rho \times \exp(\alpha + \ln(\rho \times \text{DBH}^2 \times H))$	-2.977	-	-	-	0.989	5-156

*Base diameter; **These models refer to the moist tropical forests.

Figure 4.7: General trees allometric equation

In respect to palms, arborescent ferns and cecropias the following set of computations, deriving again from Tiepolo et al. (Tiepolo et al. 2002), are employed (figure 4.8).

Stratum	Region	Fitofisionomy	Equations	R ²	DBH(cm)	Height (m)	References
Atlantic forest							
Palmeiras	Floresta Ombrófila Densa, Guaraquecaba, PR	Floresta tropical úmida (1.500-3.500 mm.ano ⁻¹) - montana	$BS = 0.3999 + 7.907 \cdot H$	0,75		1-33	Tiepolo et al. (2002)
Lianas	Floresta Ombrófila Densa, Guaraquecaba, PR	Floresta tropical úmida (1.500-3.500 mm.ano ⁻¹) - montana	$BS = 563,56 \cdot \text{DAP}^{0,6277}$	0,89	0,3 - 2,5		Tiepolo et al. (2002)
Fetos arborescentes	Floresta Ombrófila Densa, Guaraquecaba, PR	Floresta tropical úmida (1.500-3.500 mm.ano ⁻¹) - montana	$BS = -4266348 / (1-2792284 e^{-0,319772 \cdot H})$	0,88		1 - 8	Tiepolo et al. (2002) modificada por Vieira et al. (2008)
Cecropia sp	Floresta Ombrófila Densa, Guaraquecaba, PR	Floresta tropical úmida (1.500-3.500 mm.ano ⁻¹) - montana	$BS = (-0,48367 + 1,13488 \cdot (\text{Sqr}(\text{DAP})) \cdot \text{Log}(\text{DAP}))^2$	0,62		1 - 11	Tiepolo et al. (2002)

Figure 4.8: Palms, arborescent ferns and cecropias allometric equations

Regarding **PUP stand** instead, the biomass is obtained through the allometric

equation provided by Ramos et al., (Ramos et al. 2008) (figure 4.9), where the total aerial biomass is the result of leaf biomass, plus the stipe, the heart of palm and the inner sheaths of the leaves that protect the heart of palm.

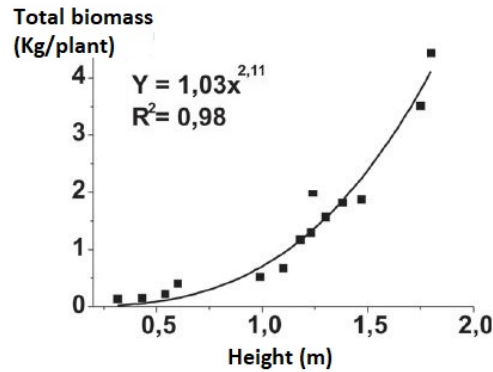


Figure 4.9: Peach palm allometric equation

Native forest

The weight of the inventoried species considering all the 7 parcels is 52'753 *Kg*. Dividing this value by the total area of the parcels, yields to 30.14 *Kg/m²*, that is the dry aboveground biomass per unit of area.

Regenerated forest

The total weight considering the 6 parcels is 42'057 *Kg*, the dry aboveground biomass per unit of area is 28.04 *Kg/m²*.

Pupunha culture

The weight of the inventoried peach palms considering the parcel area is 582 *Kg*, the dry aboveground biomass 2.33 *Kg/m²*.

According to Haag et al., (D. 1997), the value stated for Peach palm for Palmito production is 1.3 - 3.1 *Kg_{DM}/m²*, which confirms the result.

Carbon estimate

The biomass is converted into carbon content. For all stands, it's assumed as carbon fraction in biomass the rate 0.47 (carbon per biomass dry matter), assessed in Eggleston 2006.

Native forest

Multiplying the carbon fraction for the *aboveground_{DM}/m²*, it's achieved an above-ground carbon content of 14.17 *KgC/m²*.

The 'National Inventory 2020' (Oliveira Santos 2020) confirms the result with 14 *KgC/m²*.

Regenerated forest

The outcome is 13.18 *KgC/m²*.

Capellesso et al. 2020 is approximately in line, with 8 *KgC/m²*.

Pupunha culture

The outcome is 1.09 *KgC/m²*.

4.4 Root compartment

Sampling

Considering the various typologies, fragmentation, and anthropization degree of Brazilian forests, the estimation of carbon in roots is a great challenge. In addition to these factors, legal aspects have to be considered, since destructive sampling is forbidden. In fact, most of natural forests are incorporated into conservation units. Thus are alternatively exploited literature aerial-biomass/root-biomass equations.

Biomass estimate

Relating NAT and REG, the root-aerial relationship is 0.237 root dry mass/plants dry mass. For PUP, the value picked it's 0.29 root dry mass/plants dry mass.

Native forest

The total dry root biomass is 12'500 *Kg*.

Dividing it by the total area of the parcels, a dry root biomass per unit area of 7.14 *Kg/m²* is obtained.

Regenerated forest

The outcome is 6.79 *Kg/m²*.

Pupunha culture

The outcome is $0.67 \text{ Kg}/\text{m}^2$.

Carbon estimate

As for aboveground biomass, it's assumed $0.47 \text{ KgC}/\text{Kg}_{DM}$.

Native forest

Multiplying the carbon fraction for the $root_{DM}/\text{m}^2$, it's achieved a root carbon content of $3.36 \text{ KgC}/\text{m}^2$.

Regenerated forest

The outcome is $3.19 \text{ KgC}/\text{m}^2$.

Pupunha culture

The outcome is $0.32 \text{ KgC}/\text{m}^2$.

4.5 Litter compartment

Plant litter contributes significantly to soil organic matter, nutrients and mineralization through decomposition processes, maintaining site fertility and productivity. The reestablishment of this system is highly important during forest regeneration, particularly in tropical forests, where most available nutrients are bound to vegetation biomass and to organic matter of the upper soil layers (Brown and Lugo 1982).

Sampling

To quantify the litter deposited on the forest floor, a wooden frame is used, measuring $0.35 \text{ m} \times 0.35 \text{ m}$ internally (Figure 4.10).

The frame is randomly dropped six times for each parcel (three drops to the right and to the left of the transept within the 5 m lateral spacing); for each release, all the material that remains inside is collected and placed in plastic bags for subsequent analysis.



Figure 4.10: Litter measuring tool

Carbon estimate

Litter carbon quantification does not make use of allometric equations or relationships between compartments, instead it's obtained through laboratory analysis. The procedure is the same reported in paragraphs 3.3 - 3.4 for soil C&N analysis by Elementar @Vario cube.

The averages of elements percentages of all parcels are obtained. The quantity of carbon is computed as:

$$C (Kg/m^2) = \frac{dry\ weight}{frame\ area} \cdot \%C \quad (4.1)$$

Native forest

% N	% C	% H	% S
1.95	48.46	8879.07	0.13

Table 4.1: Native forest CHNS percentages

The outcome is $0.2 KgC/m^2$.

The 'National Inventory 2020' (Oliveira Santos 2020) provides $0.7 KgC/m^2$, which is an acceptably close value.

Regenerated forest

% N	% C	% H	% S
1.60	41.52	8149.02	0.14

Table 4.2: Regenerated forest CHNS percentages

The outcome is 0.19 KgC/m^2 .

Pupunha culture

The quantification is not carried out because judged negligible by visual analysis.

4.6 Necromass compartment

Sampling

Many procedures can be adopted for necromass quantification: inventory plots, strip demarcation, intercept line, adaptive cluster, point relascope, transect relascope, and guided transect. The most suitable for regions with dense vegetation is by intercept line, in which all necromass fragments crossed by an inventory line are registered (figure 4.11). The number of intersections and the diameter of each fragment at the intersection are recorded, followed by a visual analysis of the state of decomposition.

The length of the transect can be variable, depending on the heterogeneity, quantity and size of the fallen material, anyway lengths greater than 50 m do not significantly reduce the coefficient of variation; in this case a 25m transect is adopted.

Note that the method only applies to fallen material, not to standing dead trees; these latter are quantified as alive trees.

Biomass estimate

The total volume of fallen necromass is estimated by Van Wagner (Wagner 1982):

$$V = \left(\frac{1,234}{L}\right) \cdot \sum_{i=1}^n d^2 \quad (4.2)$$

Where: d = fragment diameter i at the point of intersection (cm) [$d_{min} = 2 \text{ cm}$];
 L = transect length (m); n = number of fragments found in the transect.



Figure 4.11: Necromass quantification by intercept line

The necromass weight is computed by multiplying the volume V by the basic density provided by Keller et al., (Keller et al. 2004) in figure 4.12; these values discount existing empty spaces in the inventoried material, which vary significantly according to the class of decomposition. The decomposition classes are subdivided in:

1. new material → presence of branches and intact wood texture;
2. material in initial decomposition → remains of bark, without branches and firm wood;
3. material in advanced decomposition → without bark, without branches and wood with crumbling texture.

The weight is calculated for every branch or twig in order to be able to multiply each volume by the corresponding density. The total weight of a parcel is therefore the sum of each branch or twig weight; this in order to comply with the structure of the formula reported above.

The total biomass in necromass compartment is finally computed as the average of the weights obtained from each parcel.

Diameter (cm)	Class of decomposition	Density (Mg/m ³)
< 5	-	0,36
5 a 10	-	0,45
> 10	1	0,70
	2	0,58
	3	0,28

Figure 4.12: density as function of decomposition state

Native forest

The outcome is 2.71 Kg/m^2 .

Regenerated forest

The outcome is 1.53 Kg/m^2 .

Pupunha culture

The quantification is not carried out because judged negligible by visual analysis.

Carbon estimate

For the evaluation of necromass carbon content, the rate used is 0.43 KgC/Kg_{DM} , assessed by the 'National Inventory 2020' (Oliveira Santos 2020).

Native forest

Multiplying the value above by the dry biomass per unit of area, it's achieved a necromass carbon content of 1.16 KgC/m^2 .

Regenerated forest

The outcome is 0.66 KgC/m^2 .

4.7 Total biomass carbon

The share from each compartment for each land use is shown in figure 4.13.

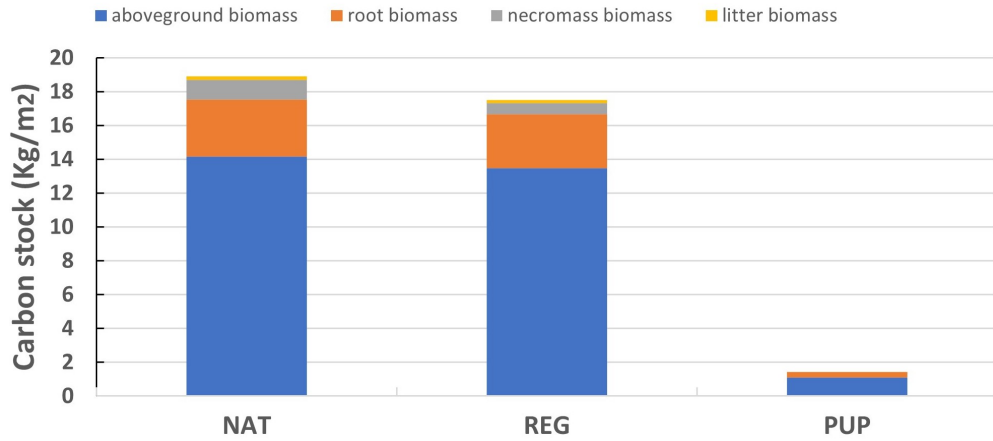


Figure 4.13: Compartments carbon stock share

The standard deviations are computed considering as argument the partial carbon contents deriving from different parcels, figure 4.14.

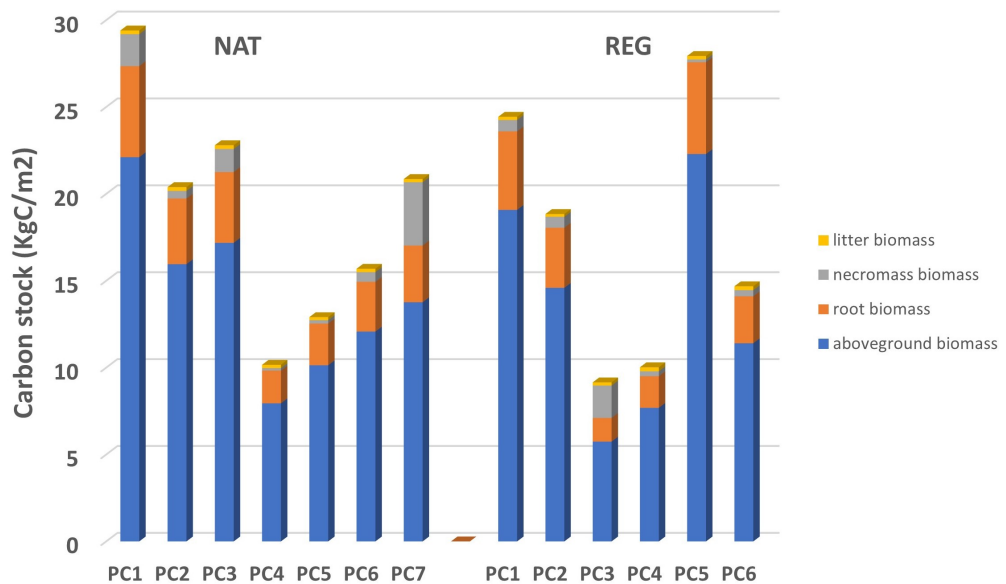


Figure 4.14: Biomass carbon stocks standard deviations

Summing the contributions of above ground, root, litter and necromass compartments, the Total biomass (TB) carbon results of table 4.3 are achieved:

Land-use	TB (KgC/m ²)	SD (KgC/m ²)
Native forest	18.90	6.51
Regenerated forest	17.50	7.65
Pupunha forest	1.41	-

Table 4.3: Total biomass carbon results

The C sequestration rate (*tC/ha/year*) is calculated as the difference with the reference native forest. REG carbon sequestration rate is computed by dividing the Δ carbon stock by 29 (years of forest succession), for PUP dividing by 24 (years since pasture introduction); figure 4.15.

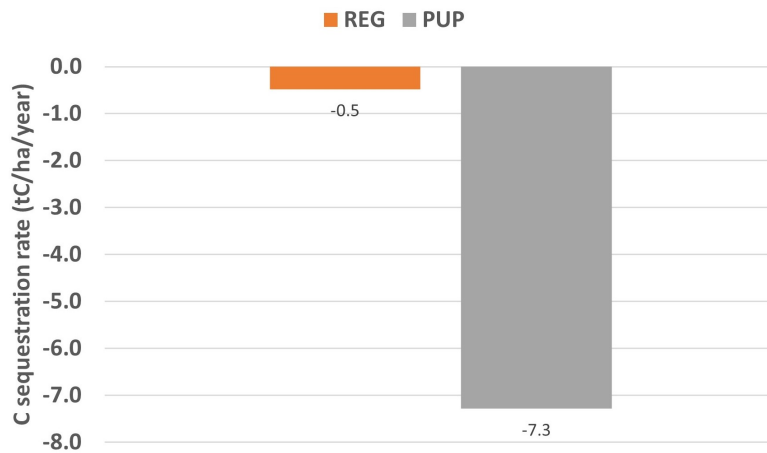


Figure 4.15: NAT-related carbon sequestration rate

The Δ C in Total biomass (Δ TB) in relation to unaltered forest, is reported in table 4.4, in *CO₂eq*.

Land-use	Δ TB (KgCO ₂ /ha/year)
Regenerated forest	-1755
Pupunha culture	-26707

Table 4.4: NAT-related Total biomass carbon in *CO₂equivalent*

4.8 Result discussion

The gained results of Total biomass carbon confirm the hypothesis of decreasing carbon stocks in relation to greater anthropization; the following observations arise:

- REG biomass carbon stock it's almost completely recovered, as can be seen from the comparison with the reference unaltered NAT.
- PUP biomass carbon stock it's very low compared to the other stands, confirming that deforestation has a high negative impact on carbon stocks.

Further comments:

- NAT and REG necromass and litter together represent 5% - 8% of the total carbon stored in inventoried forest biomass.
- The humid nature of this specific forest causes necromass values to be high compared to other biomes.
- High variance in the carbon stocks of different plots it's noticed.

Literature check

In this Chapter the outcomes validation with literature has been performed only when the latter was available, in the dedicated paragraphs.

Chapter 5

Net carbon emission

When calculating the mitigation of a system, the assessment of the mitigation potential is performed by means of the global warming potential GWP of that system (Six et al. 2004), expressed in *CO₂ equivalent*.

The Net emissions of the regenerating forest (REG) and of the Pupunha plantation (PUP) in relation to the native forest (NAT), are computed based on the contributions of the following carbon inputs/outputs:

- *CO₂eq* soil-emitted GHGs, represented by *N₂O&CH₄* fluxes (see Chapter 2);
- *CO₂eq* sequestered in soil, represented by ΔSOC (see Chapter 3);
- *CO₂eq* sequestered in vegetation, represented by ΔTB (see Chapter 4).

Net emissions are computed as:

$$N_2O + CH_4 - \Delta SOC - \Delta TB \quad (5.1)$$

5.1 Results

The carbon inputs/outputs contributions are displayed in figure 5.1.

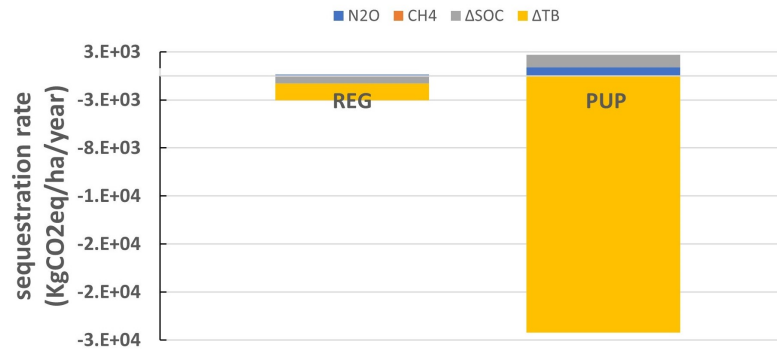


Figure 5.1: NAT-related carbon sequestration rate

The outcomes are reported in table 5.1

Land-use	Net emission ($KgCO_2/ha/year$)
Native forest	-
Regenerated forest	2575
Pupunha culture	26250

Table 5.1: Carbon net emissions of natural regenerating forests and palm cultivations, in relation to native forests, in Atlantic forest biome.

5.2 Result discussion

The Net carbon emission results confirm the hypothesis of decreasing carbon stocks in relation to greater anthropization:

- REG and PUP stands turn out to emit much more carbon to the atmosphere in relation to NAT, emphasizing the importance of environmental protection;
- REG emits 1000% less than PUP, confirming that natural regeneration has a high positive effect on carbon stocks.

General comments:

- The main contribution to carbon sequestration comes from the accumulation in plants biomass;
- The second largest contribution to carbon sequestration comes from the storage in the soil.

Chapter 6

Conclusions

The goals expressed in the introduction of this dissertation are met; the results and comparisons of carbon emissions in relation to land use transformations are provided (table 6.1).

Land-use	Net emission ($KgCO_2/ha/year$)
Native forest	-
Regenerated forest	2575
Pupunha culture	26250

Table 6.1: Carbon net emissions of natural regenerating forests and palm cultivations, in relation to native forests, in Atlantic forest biome.

Based on the interpretation of the outcomes, it's possible to formally confirm the hypothesis of decreasing carbon capture values in relation to greater anthropization. Regenerating forests and palm cultivations turn out to emit much more carbon to the atmosphere as a whole in relation to unaltered forests, emphasizing the importance of environmental protection. Additionally, the net emission from regenerated forests is one order of magnitude lower than that from cultivated field, proving the positive impact of natural regeneration on carbon stocks.

The methodology adopted in this essay falls within the Protocol endorsed by Embrapa, the state-owned research corporation affiliated with the Brazilian Ministry of Agriculture. Embrapa guidelines were not always available in a suitable form and it was missing a unified and comprehensive vision. In this way, besides the data achieved, this work offers a comprehensive review, along with some improvements included and implemented.

A future development of the present research could be the insertion of the outcomes into the Carbon market system.

” Carbon markets are trading systems in which carbon credits are sold and bought. A carbon credit is a certificate or permit representing the right to emit a set amount of carbon dioxide or the equivalent of a different greenhouse gas ($t CO_2eq$). Carbon markets are a component of international attempts to mitigate the growth in GHGs concentrations by driving industrial and commercial processes in the direction of less carbon intensive approaches.”

Carbon markets can be divided into two types: compliance and voluntary. Compliance markets are created as a result of any national, regional and/or international regulatory requirement. Voluntary carbon markets refer to the issuance, buying and selling of carbon credits on a voluntary basis. The supply of voluntary credits comes from private entities that develop carbon projects or governments that develop programs that generate emission reductions and/or removals.

The data achieved could be collocated at this point in the system. The significant difference encountered between regenerated forests and cultivated areas in terms of net carbon emissions could be the driving force of restoration programs; these can be converted into voluntary credits, potentially alleviating the funding problem of climate mitigation. Furthermore, this work demonstrates the effectiveness of natural regeneration, as regenerated forests’ outcomes are much closer to those of unaltered forests compared to agricultural cultivation.

Bibliography

- [1] Gilberto Tiepolo, Miguel Calmon, and André Rocha Feretti. *Measuring and Monitoring Carbon Stocks at the Guaraqueçaba Climate Action Project, Paraná, Brazil*. 2002 (cit. on pp. 4, 77).
- [2] Adriana Ramos, Marilene Leão Alves Bovi, and Marcos Vinícius Folegatti. *Estimativas da área foliar e da biomassa aérea da pupunheira por meio de relações alométricas*. 2008 (cit. on pp. 4, 78).
- [3] HS Eggleston. *Estimation of Emissions from CO₂ Capture and Storage: the 2006 IPCC Guidelines for National Greenhouse Gas Inventories*. 2006 (cit. on pp. 4, 29, 68, 78).
- [4] C E Van Wagner. «Practical aspects of the Line intersect method». In: (1982) (cit. on pp. 4, 82).
- [5] Michael Keller, Michael Palace, Gregory P. Asner, and Rodrigo Pereira. «Coarse woody debris in undisturbed and logged forests in the eastern Brazilian Amazon». In: *Global Change Biology* (2004) (cit. on pp. 4, 83).
- [6] Mauro Meirelles de Oliveira Santos. *Projeto BRA/16/G31 Quarto Inventário Nacional de emissões e remoções antropicas de gases de efeito estufa*. 2020 (cit. on pp. 4, 79, 81, 84).
- [7] Takahiko Hiraishi, Thelma Krug, and Kiyoto Tanabe. «2013 Supplement to the 2006 IPCC Guidelines for National Greenhouse Gas Inventories: Wetlands». In: (2014) (cit. on pp. 6, 55).
- [8] *Global Forest Resources Assessment (FRA)*. FAO, 2020 (cit. on pp. 16, 18, 72).
- [9] Angelo Sartori. *Estrategia Nacional de Bosques y Cambio Climático (ENBCC) de Chile*. 2018 (cit. on p. 16).
- [10] Máisa Guapyassú and Gustavo Adolfo Gatti. *Plano de manejo da Reserva natural Salto Morato - Guaraqueçaba (PR)*. 2011 (cit. on p. 17).

- [11] Henrique Pimenta Veloso, Antonio Lourenço Rosa Rangel Filho, and Jorge Carlos Alves Lima. *Classificação da vegetação brasileira, adaptada a um sistema universal*. Ministério da Economia, Fazenda e Planejamento, Fundação Instituto Brasileiro de Geografia e Estatística, Diretoria de Geociências, Departamento de Recursos Naturais e Estudos Ambientais, 1991 (cit. on p. 18).
- [12] IBGE Fundação Instituto Brasileiro de Geografia e Estatística. *Manual técnico da vegetação brasileira*. 1992 (cit. on p. 18).
- [13] Maurício Bergamini Scheer. *Decomposicao e liberacao de nutrients da Serapilheira foliar em I'm trecho de Floresta Ombrofila Densa Aluvial em Regeneracao, Guaraquecaba (PR)*. 2008 (cit. on p. 20).
- [14] Timothy Pearson, Sarah Walker, and Sandra Brown. *Sourcebook for Land use, Land-use change and Forestry Projects*. 2005 (cit. on p. 28).
- [15] Richard Birdsey, Kurt Pregitzer, and Alan Lucier. «Forest Carbon Management in the United States: 1600-2100». In: *Journal of Environmental Quality* (2006) (cit. on p. 29).
- [16] Cecile de Klein and Mike Harvey. *Nitrous Oxide Chamber Methodology Guidelines*. Ministry for Primary Industries, New Zealand, 2015 (cit. on p. 32).
- [17] Gang Liu and Bing C. Si. «Multi-layer diffusion model and error analysis applied to chamber-based gas fluxes measurements». In: *Agricultural and Forest Meteorology* (2009) (cit. on p. 33).
- [18] Rafael Geha Serta. *Avaliacao de criterios metodologicos de coleta de gases de efeito estufa emitidos a partir do solo*. 2013 (cit. on p. 35).
- [19] Timothy B. Parkin and Rodney T. Venterea. *USDA-ARS GRACEnet Project Protocols. Chamber-Based Trace Gas Flux Measurements*. 2010 (cit. on p. 42).
- [20] Rodney T. Venterea, Kurt A. Spokas, and John M. Baker. «Accuracy and Precision Analysis of Chamber-Based Nitrous Oxide Gas Flux Estimates». In: *Soil Science Society of America Journal* (2009) (cit. on p. 49).
- [21] T. B. Parkin, R. T. Venterea, and S. K. Hargreaves. «Calculating the Detection Limits of Chamber-based Soil Greenhouse Gas Flux Measurements». In: *Journal of Environmental Quality* (2012) (cit. on p. 49).
- [22] Sirwan Yamulki, K.W.T. Goulding, C.P. Webster, and Roy M. Harrison. *Studies on NO AND N₂O fluxes from a wheat field*. 1995 (cit. on p. 50).
- [23] L. M. Cardenas, R. Thorman, N. Ashlee, M. Butler, and D. Chadwick. «Quantifying annual N₂O emission fluxes from grazed grassland under a range of inorganic fertiliser nitrogen inputs». In: *Agriculture, Ecosystems and Environment* (2010) (cit. on p. 50).

- [24] Reginaldo Barboza da Silva, Taline Antunes, Jéssica Silva Rosa, and Ana Paula Packer. « CO_2 , CH_4 and N_2O emissions after fertilizer application in banana plantations located in the Brazilian Atlantic Forest». In: *Soil Use and Management* (2022) (cit. on p. 57).
- [25] Josiléia Acordi Zanatta, Karina Pulrolnik, João Herbert, and Moreira Viana. «Protocolo para avaliação do estoque de carbono e de nitrogênio do solo em sistemas florestais – Projeto Saltus». In: (2015) (cit. on p. 58).
- [26] Guilherme Kangussú Donagema, David Vilas Boas de Campos, and Sebastião Barreiros Calderano. «Manual de Métodos de Análise de Solo». In: (2011) (cit. on p. 59).
- [27] B H Ellert and J R Bettany. *Calculation of organic matter and nutrients stored in soils under contrasting management regimes*. 1995 (cit. on p. 68).
- [28] Claudia P.J. Sisti, Henrique P. Dos Santos, Rainoldo Kohhann, and Bruno J.R. Alves. «Change in carbon and nitrogen stocks in soil under 13 years of conventional or zero tillage in southern Brazil». In: (2004) (cit. on p. 68).
- [29] Murilo Gomes Veloso, Jeferson Dieckow, Josiléia Acordi Zanatta, and Cimelio Bayer. «Reforestation with loblolly pine can restore the initial soil carbon stock relative to a subtropical natural forest after 30 years». In: *European Journal of Forest Research* (2018) (cit. on p. 72).
- [30] Haag D. *Root distribution patterns in a polycultural system with local tree crops on an acid upland soil in central Amazonia*. 1997 (cit. on p. 78).
- [31] Elivane Salete Capellesso, Anamaria Cequinel, and Renato Marques. «Temporal and environmental correlates of carbon stocks in a regenerating tropical forest». In: *Applied Vegetation Science* (2020) (cit. on p. 79).
- [32] Sandra Brown and Ariel E Lugo. *The Storage and Production of Organic Matter in Tropical Forests and Their Role in the Global Carbon Cycle*. 1982 (cit. on p. 80).
- [33] Johan Six, Stephen M. Ogle, F. Jay Breidt, Rich T. Conant, and Arvin R. Mosiers. «The potential to mitigate global warming with no-tillage management is only realized when practised in the long term». In: *Global Change Biology* (2004) (cit. on p. 88).